








The structural framework of the north-central Guiana Shield: a fossil fold-and-thrust belt in northeastern Roraima state, Brazil

Túlio A. A. Mendes¹, Antonio C. S. Oliveira¹, Marcelo E. Almeida², Fabrício A. Caxito³,
Tiago A. Novo³

¹Geological Survey of Brazil, CPRM-SUREG-MA, Av. André Araújo 2010, Manaus-AM, Brazil, CEP: 69067-375

²Geological Survey of Brazil, CPRM-ERJ, Avenida Pasteur, 404, Urca, Rio de Janeiro-RJ, Brazil. CEP: 22290-255

³Universidade Federal de Minas Gerais - UFMG, Geology Department – Institute of Geosciences, CPMTCC-IGC, Belo Horizonte-MG, Brazil, CEP: 31270-901

Abstract

The northeastern Roraima state (Brazil), located in the north-central portion of Guiana Shield, shows shallow-granitoids and associated volcanic rocks of the Orocaima Igneous Belt (2.00-1.96 Ga) overlaid by the Arai Formation sedimentary succession (1.96-1.87 Ga). Previous authors suggested a compressional event affecting the region. Meanwhile, recent papers interpreted that transpressional deformation, related to a distal effect of a Late Mesoproterozoic tectonics (K'Mudku Event), reactivated some basement structures and generated drag folds in the supracrustal successions. This paper presents a multi-scale approach to the best-exposed sector of this geological framework, gathering and analyzing new data from the regional photointerpretation to the thin section scales. The structural data reveal the fractal character and the rheological control on the E-W- and ESE-WNW-trending compressional structures. The southern domain presents sub-vertical shear zones with down-dip to oblique lineation, which are related to the uplift of the shallow-granitoids in relation to the coeval volcanic successions. The central domain, where the volcanic succession crops out, exhibits ubiquitous E-W- to ESE-WNW-trending sub-vertical foliation parallel to the axial plane of the folds. The southern border of the northern domain (Arai Formation) shows spaced cleavage and gentle folds, besides sub-horizontal thrust faults. The structures reveal a fold-and-thrust belt that presents a transition from thick- to thin-skinned tectonics with mass transport to the north. These geometric relations do not match with the K'Mudku lineaments, usually following a NE-SW direction in the north-central Guiana Shield. However, the southward Middle Orosirian structural framework (Uatumã-Anauá Domain) shows similar geometric relations with nearly E-W-trending lineaments and parallel sub-vertical foliation.

Article Information

Publication type: Research Papers
Received 29 June 2021
Accepted 27 December 2021
Online pub. 7 January 2022
Editor: Evandro Klein

Keywords:
northeastern Roraima,
multi-scale structural approach,
fractal,
geometric relations.

*Corresponding author
Túlio A. A. Mendes
tulio.mendes@cprm.gov.br

1. Introduction

The north-central Guiana Shield preserves shallow crustal rocks, generated during the Middle to Late Orosirian, which are represented by the Roraima Supergroup volcano-sedimentary sequences and their basement. These basement rocks consist of widely dispersed volcanic successions and associated shallow-granitoids (Orocaima Igneous Belt). According to the current tectonic interpretation, the Orocaima Igneous Belt's magmatism is related to a post-collisional setting (Fraga et al. 2017a, 2018), and the Roraima Supergroup comprises the record of a rift-sag basin (Reis et al. 2017). During a Late Mesoproterozoic intracontinental tectonics, the K'Mudku Event (ca. 1.49-1.15 Ga; Santos et al. 2006b), these successions recorded partial positive inversion due to uplift and lateral escape tectonics. Therefore, they promote

the reactivation of pre-existing normal faults associated with far-field intraplate stresses derived from collisional tectonics at the edge of the continent (Pinheiro et al. 1990; Fraga et al. 2017b; Reis et al. 2017). Nevertheless, the tectonic evolution in the north-central Guiana Shield remains a contentious topic, as the structural architecture was not still clearly set out and evaluated in more detailed studies.

Deformational structures comprising folding, thrust faults, and solid-state foliation with a high-rake mineral stretching lineation, disposed along a wide and elongated area, can be intuitively related to crustal shortening in a fold-and-thrust belt (McQuarrie and Ehlers 2017; Butler et al. 2018). However, the definition of the driving forces (i.e., compressive plate boundaries, such as subduction, collisional or transpressional zones, or far-field intraplate stress propagation) responsible for deformation can be challenging to determine (Poblet and



Lisle 2011), especially in regions with significant gaps of basic geological mapping. In fact, the characterization of the structural framework provides the basis for understanding the tectonic fossil record.

The purpose of this paper is the study of a set of structures present in the central Orocaina Igneous Belt and their immediate overlying sedimentary succession, the Arai Formation (basal unit of the Roraima Supergroup), which composes the geological framework of the northeastern Roraima state (Brazil). From the regional photointerpretation (i.e., SRTM and aerogeophysical images), field work and petrological/microstructural analysis, a multi-scale approach reveals the typology and fractal character of the deformational structures. The variety of lithotypes (e.g., metagranitoids, coherent metavolcanic and metavolcanoclastic rocks, and sandstones) and their intrinsic rheological features promote the strain partitioning and differences in structural patterns. Then, based on the available literature data, it was discussed herein the tectonic events that may have generated this structural framework.

2. Geological background

2.1 Tectonic overview

Guiana Shield is a large Precambrian cratonic area corresponding to the northern Amazon Craton. Several geochronological models were proposed for this craton as isotopic analytical techniques were applied to perceive this under-mapped region (e.g., Tassinari and Macambira 1999, 2004; Santos et al. 2000, 2006a, 2008; Cordani and Teixeira 2007 – Figure 1A). These models are very comprehensive and use geochronological and isotopic data to propose different geochronological provinces that constitute the craton, but recent publications offer in-depth tectonic interpretations for the study area (north-central Guiana Shield).

Fraga et al. (2008, 2009, 2017c) report a nearly east-west sinuous mega-structure extending from the northwestern Roraima state (Brazil) to the southwestern Suriname, formed by high-grade supracrustal rocks and generated during a collisional tectonic phase (Caurane-Coeroene Belt; 2.02-2.00 Ga – Figure 1B). Northward to this belt and covering an even more extensive area, the Orocaina Igneous Belt presents two volcano-plutonic associations whose crystallization ages range from 2.00 to 1.96 Ga. Based on the alkaline and high-K calc-alkaline chemical signature of these rocks, Fraga et al. (2017a, 2018) interpret a post-collisional tectonic setting for this magmatism. In the central Guiana Shield, the Rio Urubu Igneous Belt presents similar chemistry but slightly younger crystallization ages (ca. 1.96-1.91 Ga), and a complex structural pattern. According to the same authors, this belt was generated during a post-collisional transpressional event southward to the Caurane-Coeroene Belt. On the other hand, Santos et al. (2004) correlate the Creporizão (Tapajós Domain) and Pedra Pintada (Orocaina Igneous Belt) suites, suggesting a continental magmatic arc at ~1.97 Ga (Mundurucus Orogeny) in Tapajós-Parima Province.

Teixeira et al. (2019) and Barbosa et al. (2021) considered the Orocaina Igneous Belt a silicic large igneous province (SLIP; sensu Bryan and Ernst 2008). The lithochemistry (intermediate to acid) and the significant large geographic occurrence are considered to support the Orocaina SLIP interpretation. Other intraplate magmatic events also occur

in the central Guiana Shield (Figure 1B). The Uatumã SLIP (Klein et al. 2012 and references therein) includes acid to intermediate magmatic rocks along an extensive area of the central Amazon Craton, including the south-central Roraima state. In the northern Roraima and part of Venezuela and Guyana, Reis et al. (2013) interpret the voluminous dykes and sills of the Avanavero magmatism (1.79-1.78 Ga) as the record of a large igneous province (LIP; sensu Bryan 2007), which intrudes the supracrustal rocks of the Surumu Group and the Roraima Supergroup.

Furthermore, this Orosirian crust has not remained inert over geological time. Barron (1966) reports a shear event that affected the Guyana's basement rocks at ca. 1260 Ma, which he denominated as the "K'Mudku Mylonite Episode". Santos et al. (2008) defined the K'Mudku Intracontinental Orogen as an ENE-WSW elongated belt that crosses the central Guiana Shield. The geochronological data of some metamorphic rocks of the region (Ar-Ar dates in phyllosilicates and U-Pb dates in titanite and zircon) record ages between 1.49 and 1.15 Ga that reveal the thermal effects chronologically correlated to the Grenvillean-aged Sunsás and Putumayo orogenies (Santos et al. 2006a, 2006b; Ibanez-Mejía et al. 2011; Oliveira et al. 2019).

2.2 Orosirian supracrustal successions and related granitoids of northeastern Roraima state (north-central Guiana Shield)

The lithological products of the Orocaina Igneous Belt comprise the basement rocks in the study area, which is represented by two main volcano-plutonic associations. Based on chemical and geochronological (Table 1) data, Aricamã and Pedra Pintada suites, including the related volcanic rocks, such as the Cachoeira da Ilha Formation and Surumu Group, respectively, were considered as produced by post-tectonic magmatic events. These events succeeded the Transamazonian tectonics – Trairão-Anauá arc system – during the Paleoproterozoic era (Fraga et al. 2017a, 2018).

The Pedra Pintada Suite contains greyish granitoids (i.e., granite, granodiorite, tonalite, and quartz diorite). According to a near east-west trend, these granitoids occur continuously over large sites in the northern Roraima (Fraga et al. 1996, 1997). The Surumu Group includes andesites, dacites, rhyolites, ignimbrites, subvolcanic, and volcanogenic sedimentary rocks with the same composition (Fraga et al. 2010). This magmatic association presents high-K calc-alkaline chemical affinity and crystallization ages between 1991 ± 18 Ma and 1956 ± 5 Ma (Table 1). Meanwhile, Amaral (1974) and Teixeira (1978) present isotopic data based on low-temperature systems (K-Ar whole-rock and in amphibole analyses) with ages between 1263 ± 47 Ma and 721 ± 36 Ma.

The Aricamã Suite gathers the oldest granitoids of the Orocaina Igneous Belt (Table 1). These rocks are found in isolated plutonic bodies composed of pinkish syenogranites and alkali-feldspar granites, presenting xenomorphic mafic mineralogy (biotite \pm hornblende) and indicating late crystallization from an anhydrous magma (Fraga et al. 2009). The Cachoeira da Ilha Formation volcanic rocks are ignimbrites, coherent rhyolites arranged in lenticular bodies, and acidic subvolcanic rocks that occur as dikes cross-cutting the Surumu Group and Pedra Pintada Suite (Fraga et al. 2010). The analytical data of this magmatic association reveals an affinity with A-type granites with crystallization ages between 2007

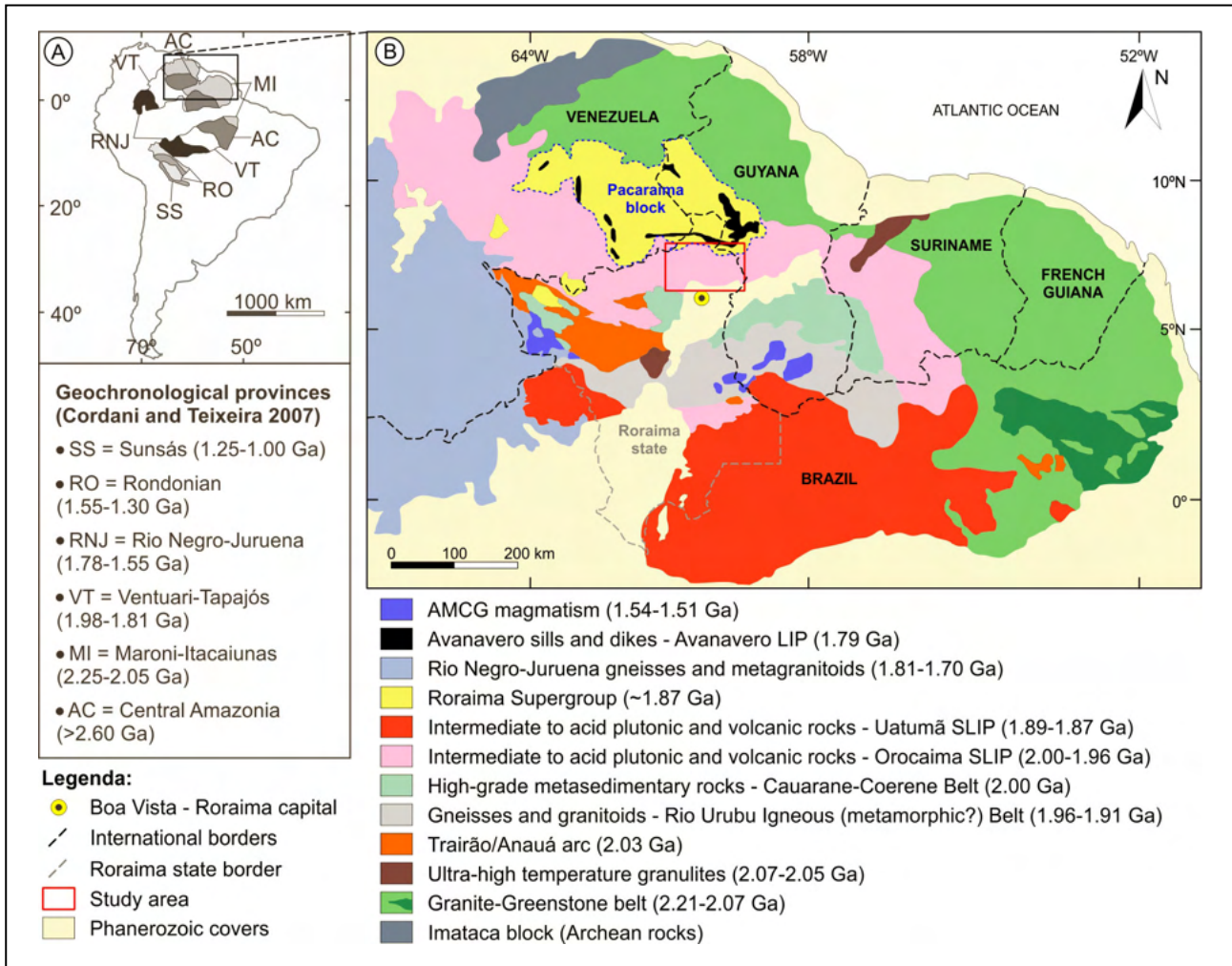


FIGURE 1. Schematic tectonic map of the central and eastern Guiana Shield. (A) Location map containing the tectonic provinces of the craton, according to the geochronological model of Cordani and Teixeira (2007). (B) Modified figure from Reis et al. (2021a), based on the data compilation of Fraga et al. (2009, 2017c), Klein et al. (2012), Reis et al. (2013), and Teixeira et al. (2019). A red polygon highlights the study area.

± 3 Ma and 1986 ± 4 Ma (Table 1). It is highlighted herein a noteworthy temporal disparity, as the Aricamã-Cachoeira da Ilha magmatic association presents older crystallization ages than the Pedra Pintada-Surumu magmatic association, contrasting with the field relations described by Fraga et al. (2010).

The Roraima Supergroup is a volcano-sedimentary sequence with predominance of siliciclastic rocks (Pinheiro et al. 1990). According to Reis et al. (2017), a north-south-trending extensional event leads to an Orosirian rift-sag basin opening (1.95-1.78 Ga). The Arai Formation is the basal succession of this basin and includes (conglomeratic) sandstones, conglomerates, and mudstones that lay discordantly above the Surumu Group volcanic rocks. The detrital zircon record of the Arai Formation reveals a younger population at 1958 ± 19 Ma (youngest peak age in histogram plot) and the presence of tuff layers dated 1873 ± 3 Ma (Santos et al. 2003; Table 1), deposited in an overlying formation (Uaimapué), restrict the Arai sedimentation age to the 1.96-1.87 Ga interval.

2.3 Structural framework reports in the literature

Based on a photointerpretation study, Bonfim et al. (1974) firstly refer to “mega folds” in the Surumu Group. They also

described volcanic rocks with dynamo-metamorphic texture, related to their characteristic outcrop features of sharp-edged sub-vertical plates. However, for these authors the folds resulted from volcanic accommodation in the irregular paleogeography (i.e., primary features). Therefore, based on this conception, the solid-state foliation would not be related to the arrangement of the fold-like layers resulting from a later tectonic event.

Other studies (Pinheiro et al. 1990; Costa et al. 1991; Fraga et al. 1994a, 1994b, 2010) bring more detailed information on the deformational features of the volcanic basement and the Arai Formation. These authors outline an E-W to WNW-ESE structural trend (i.e., structural lineaments, shear zones, and secondary foliation) that controls part of the supracrustal rocks of the northeastern Roraima state. A steep northward dipping foliation, parallel to the folds' axial plane, contains a high-rake mineral stretching lineation. Some authors assigned these deformational features to the K'Mudku Intracontinental Orogeny (i.e., Santos et al. 2000). However, studying the volcanic rocks of the region, Barbosa (2020) and Barbosa et al. (2021) described only rheomorphic folds and interpreted that most of the succession, at least in the central portion of the Orocaima Igneous Belt, is preserved from tectonic deformation.

TABLE 1. Geochronological data of the study area geological units.

Geological unit	Lithotype	Reference (n) and method	Age (Ma)
Avanavero	Dolerite	(2) K-Ar in whole rock	1574 ± 60
Avanavero	Gabbro	(1) K-Ar in whole rock	1635 ± 60
Avanavero	Dolerite	(2) K-Ar in whole rock	1757 ± 81
Avanavero	Dolerite	(1) K-Ar in whole rock	1891 ± 69
Avanavero	Dolerite	(7) U-Pb SHRIMP in zr	1782 ± 3
Avanavero	Dolerite	(7) U-Pb SHRIMP in bdy	1787 ± 14
Avanavero	Dolerite	(10) U-Pb ID-TIMS in bdy	1795 ± 2
Uaimapuê Fm. (Roraima S.)	Red ash tuff	(7) U-Pb SHRIMP in zr	1862 ± 15#
Uaimapuê Fm. (Roraima S.)	Felsic tuff	(7) U-Pb SHRIMP in zr	1873 ± 3
Arai Fm. (Roraima S.)	Conglomeratic sandstone	(7) U-Pb SHRIMP in zr	1958 ± 19YDG
Pedra-Pintada Suite	Granite	(1) K-Ar in amph	1113 ± 91
Pedra-Pintada Suite	Syenogranite	(1) K-Ar in whole rock	1263 ± 47
Pedra-Pintada Suite	Syenogranite	(6) Pb evaporation in zr	1875 ± 48
Pedra-Pintada Suite	Monzogranite	(8) U-Pb SHRIMP in zr	1956 ± 5
Pedra-Pintada Suite	Chl-hbl granodiorite	(11) U-Pb SHRIMP in zr	1968 ± 5
Pedra-Pintada Suite	Bt monzogranite	(13) U-Pb SHRIMP in zr	1969 ± 5
Pedra-Pintada Suite	Hbl-bt monzogranite	(11) U-Pb SHRIMP in zr	1971 ± 5
Pedra-Pintada Suite	Cpx-hbl quartz-diorite	(9) Pb evaporation in zr	1985 ± 1
Pedra-Pintada Suite	Hbl-bt granodiorite	(9) U-Pb LA-ICP-MS in zr	1991 ± 18
Pedra-Pintada Suite	Hbl-bt monzogranite	(9) Pb evaporation in zr	2009 ± 2*
Pedra-Pintada Suite	Bt monzogranite	(4) Pb evaporation in zr	2005 ± 45*
Surumu Group	Rhyolite	(1) K-Ar in whole rock	721 ± 36
Surumu Group	Rhyolite	(1) K-Ar in whole rock	1102 ± 57
Surumu Group	Rhyolitic ignimbrite	(11) U-Pb SHRIMP in zr	1964 ± 7
Surumu Group	Rhyodacite	(3) U-Pb ID-TIMS in zr	1966 ± 9
Surumu Group	Ignimbrite	(11) U-Pb SHRIMP in zr	1967 ± 7
Surumu Group	Rhyolite	(12) U-Pb LA-ICP-MS in zr	1980 ± 7
Surumu Group	Rhyodacite	(7) U-Pb SHRIMP in zr	1984 ± 9
Surumu Group	Ignimbrite	(9) Pb evaporation in zr	1990 ± 3
Surumu Group	Felsic volcanic rock	(5) Pb evaporation in zr	2006 ± 4*
Aricamã Suite	Syenite	(2) K-Ar in whole rock	924 ± 10
Aricamã Suite	Syenite	(11) U-Pb SHRIMP in zr	1982 ± 4
Aricamã Suite	Alkali feldspar granite	(9) U-Pb SHRIMP in zr	1986 ± 4
Aricamã Suite	Alkali feldspar granite	(9) U-Pb LA-ICP-MS in zr	1993 ± 11
Cachoeira da Ilha Formation	Rhyolitic ignimbrite	(9) Pb evaporation in zr	1990 ± 5
Cachoeira da Ilha Formation	Rhyolite	(12) U-Pb ICP-MS in zr	2002 ± 4
Cachoeira da Ilha Formation	Eutaxitic lapilli-tuff	(12) U-Pb ICP-MS in zr	2007 ± 3

References (n): 1 - Amaral (1974); 2 - Teixeira (1978); 3 - Schobbenhaus et al. (1994); 4 - Almeida et al. (1997); 5 - Costa (1999); 6 - Costa et al. (2001); 7 - Santos et al. (2003); 8 - Santos (2003); 9 - Fraga et al. (2010); 10 - Reis et al. (2013); 11 - Fraga et al. (2017b); 12 - Barbosa (2020); and 13 - Reis et al. (2021b). The asterisks beside the age values means: YDG = youngest detrital age record; * = heritage age; # = single grain apparent age. Mineral abbreviations: amph = amphibole; bdy = baddeleyite; bt = biotite; chl = chlorite; cpx = clinopyroxene; hbl = hornblende; zr = zircon. This table does not gather the data of the correlated geological units of Brazil's neighboring countries.

Fraga et al. (2017b) interpret that the solid-state foliation and folds imprinted on these supracrustal successions were generated from low to moderate temperature conditions, probably related to the reactivation of basement structures during the K'Mudku Event. Transpressive shear zones concentrated strain in bands across the volcanic and sedimentary successions, deforming also the borders of the associated granitoids. Mylonites were developed along these shear zones. Meanwhile, spaced-cleavage related folds are sometimes associated with the Surumu Group, Cachoeira da Ilha Formation, and the basal sedimentary rocks of the Roraima Supergroup.

Regarding only the Roraima Supergroup, Pinheiro et al. (1990) relate en echelon and gentle folds located in the southern border, restricted to the Arai Formation. However,

they found no record of compressive deformation in the central portion of the basin (e.g., Roraima Mount), where the supergroup's overlying sequences crop out (Pinheiro et al. 1990). Approaching the Tepequém mountain, where volcanic and siliciclastic rocks crop out nearby the study area, Luzardo (2006) described a suite of structures related to regional metamorphism (e.g., flattened quartz pebbles, axial-plane foliation, crenulation cleavage, mega folds) and suggests the existence of a post-Transamazonian collisional event with possible correlation to the K'Mudku Event (Santos et al. 2006b). However, some authors interpreted that this intracontinental event just promoted the reactivation of pre-existing basement-related faults and generated forced and drag folds in the basal layers of the Roraima Supergroup (Fernandes Filho et al. 2012; Fraga et al 2017b; Reis et al. 2017).

3. Methods

Geological and structural interpretation of geophysical and remote sensing images is routine in geological mapping, identifying the surface (and/or subsurface) response to the structural elements. The integrated analysis of multiple sensors reduces the ambiguity inherent in any interpretation, considering the image acquisition characteristics and the measured physical properties. In this paper, the methodological approach comprises the previous interpretation of the different layers using the logical-systematic methods (Guy 1966) and structural-geophysical analysis (Jessell and Valenta 1996). The geomorphological and geophysical structural interpretations were then compared with the pre-existing geological data (Figure 2).

The multi-source data sets were interpreted at 1:250.000 scale within a geographic information system platform using the Geocentric Reference System to America's Datum 2000 (SIRGAS.2000) Polyconic projected coordinate system. The approach to structural interpretation considers five main layers: (1) airborne magnetometric and (2) gamma-spectrometric; (3) DEM-SRTM; (4) LANDSAT 8 ETM+, and (4) regional geological data compiled at 1:500.000 scale.

The Surumu Aerogeophysical Project, executed by the Geological Survey of Brazil and available at GEOSGB-CPRM portal (<https://geosgb.cprm.gov.br/>), provides the airborne magnetometric and gamma-spectrometric data. The airplane survey occurred in 1976, with a north-south flight line spaced from approximately 1 km, with a one-second sampling interval (fiducial = 110 m). Firstly, with the support of the Oasis Monjat software Geosoft®, the data were reprojected, gridded in 250 m cell size, and micro-levelled. Afterward, gaussian bandpass filters (Jacobsen 1987; Oliveira 2008) were applied in magnetic anomaly field data, using parameters defined by the average radial power spectrum (Spector and Grant 1970). These previous steps allow to enhance deep and shallow sources, using parameters defined by the analysis of the average radial

power spectrum, which result in the regional (>20 km) and residual (20-0.8 km) magnetics grids.

Google Earth Engine platform (<https://earthengine.google.com/>) provides the DEM-SRTM and LANDSAT 8 OLI images. Other images (shaded relief, slope, composition, and fusions) were obtained using the ArcMap software ESRI® environment SIG. These images are the basis of the geomorphological interpretation of the geological structures assignment.

The Geological Survey of Brazil database also provides the geological information (i.e., outcrop description, geological reports, and interpretations) for the study area. Using the ArcMap software ESRI®, the outcrop stations were reclassified as rock-types (plutonic, volcanic, mafic, and mylonite/cataclasite) and pinnacle-shaped outcrop highlighted, considering the characteristic exposure of deformed and silicified rocks in the region.

4. Results

4.1 Regional structures interpretation: satellite and aerogeophysical images

The structural interpretation considers that the planar geological features (i.e., foliation, bedding, shear zones, faults, and fractures) have a linear expression in remote and geophysical sensors, assuming a contrast among the measured physical properties.

The airborne magnetometric data exhibit a homogeneous texture, and the east-west-trending anastomosed traces predominate (Figure 3A). However, the magnetic intensity increases in the southern portion, so it is possible to individualize two domains concerning the differences in magnetic sources' depths. Internally, these domains present a magnetic grid (T1) related to the trajectory of magnetic features (lineaments, anomalies, and magnetic texture), which draw tight and isoclinal folds with E-W-trending axial planes. Elongated NNE lineaments (magnetic and non-magnetic) overlap T1 and represent faults and mafic dikes (Figure 3C).

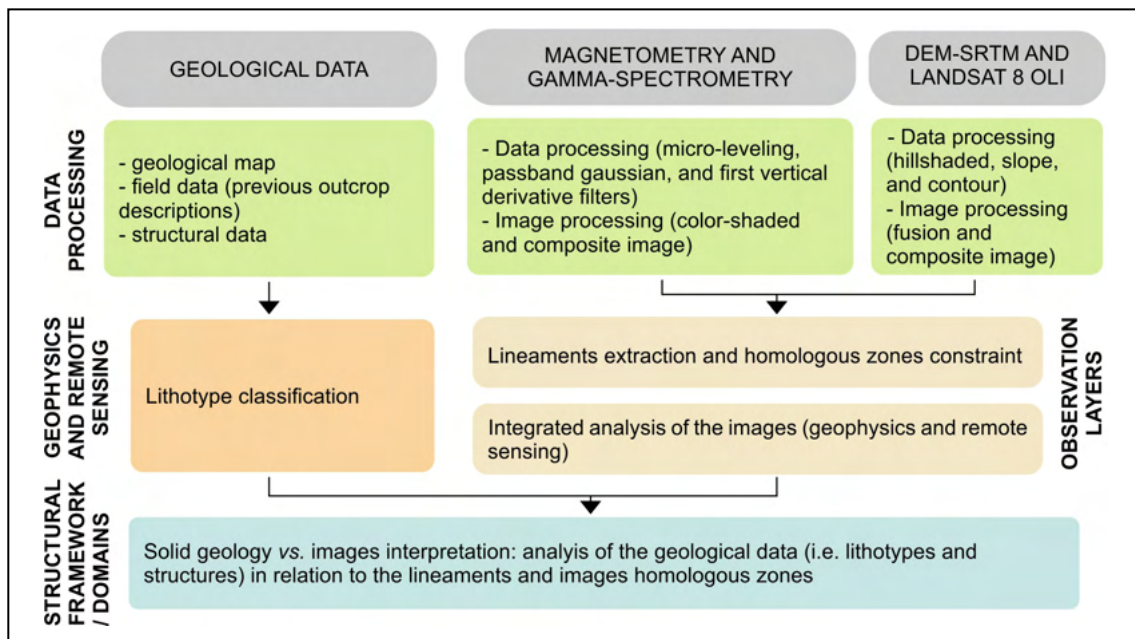


FIGURE 2. Methodological flow chart of the geological-structural modeling based on multi-source data sets.

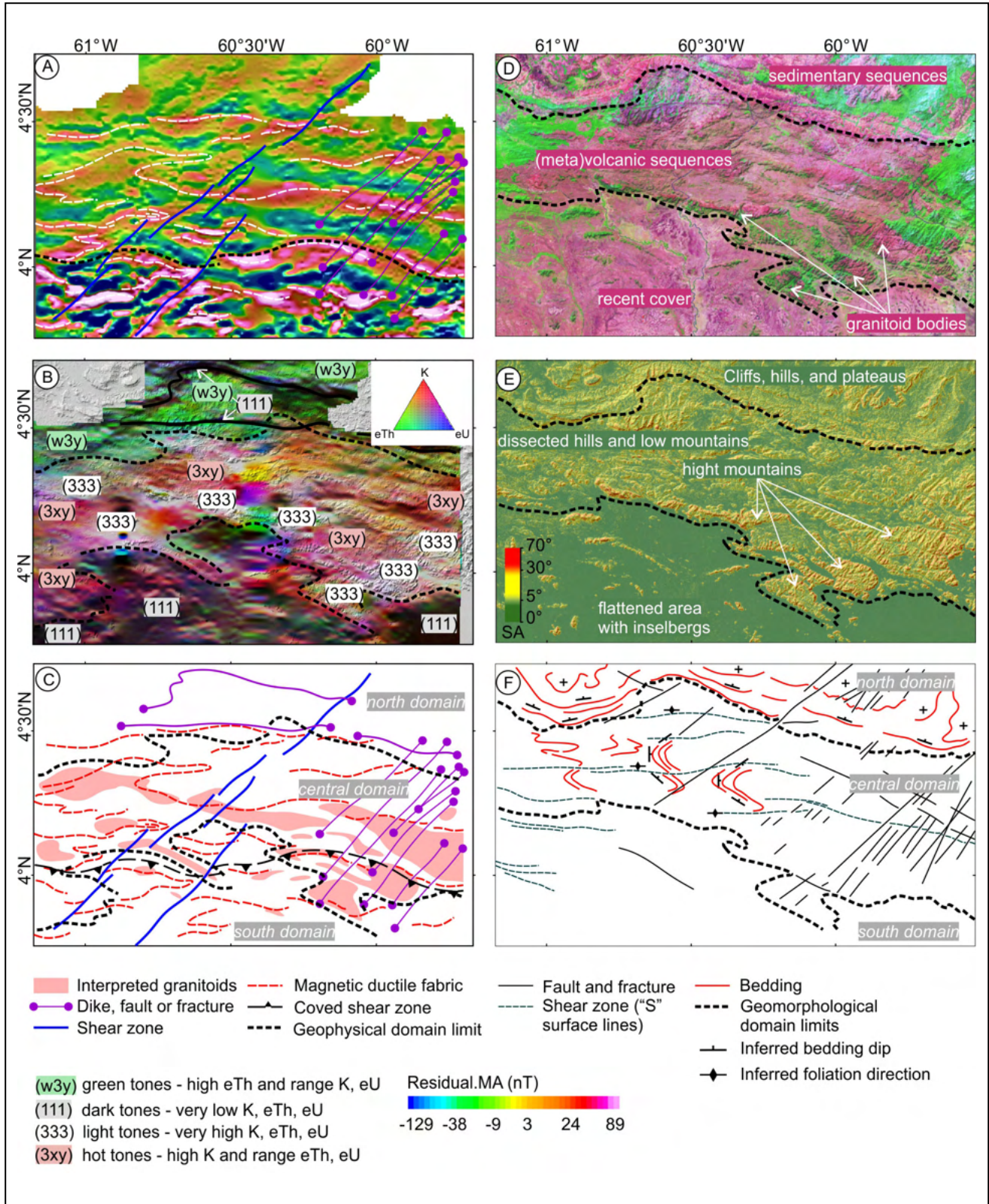


FIGURE 3. Structural interpretation of geophysical and remote sensing images. (A) Airborne magnetometric treated image; (B) RGB ternary composition image obtained from the airborne gamma spectrometric data; (C) geological and structural interpretations of the geophysical data; (D) multispectral (LANDSAT ETM 8) image; (E) topographic (MDE SRTM) image; (F) structural interpretation of the remote sensing images.

The airborne gamma spectrometric data allows evaluating the concentrations of potassium (K) and equivalent thorium (eTh) and uranium (eU) expressed in the colors of the RGB ternary composition image. In the northern Roraima three different domains were interpreted (Figure 3B and 3C): southern, central, and northern. The southern domain exhibits dark-tone colors, with spots in warm and subordinately light tones, representing low concentrations in the gamma spectrometric channels. The central domain shows warm tones representing high-K and varied eTh and eU concentrations. This domain also contains light-tone subdomains with elongated semi-elliptical shapes that follow an E-W-trending direction. The northern domain presents high-Th concentrations about the other gamma spectrometric channels, assigning colors in green tones, and shows bands with dark colors and yellow spots.

The remote sensing data - multispectral (LANDSAT ETM 8) and topographic (MDE SRTM) images - reveal three main domains based on differences of relief texture, slope angle (SA), and morphological structure (Figure 3D, 3E, and 3F). The southern domain presents a flattened relief, conserved, and degraded/retouched (SA = 0° to 5°), also showing inselbergs and other reliefs (SA = 20° to 90°). The flattened relief is associated with recent sedimentary coverings while the inselbergs and steeper reliefs are related to the plutonic bodies and deformed volcanic layers with WNW-ESE direction. The central domain comprises dissected hills, hills, and low mountains (SA = 5° to 35°). Subordinately, this domain also has elongated semi-elliptical portions with high mountain relief (AIT = 25° to 90°). The dissected hill and low mountains are correlated with folded volcanic successions and the high mountains are associated with granitoid rocks. The morphological structures in this domain are related to folded ridges with an E-W-trending axial plane and the dissected areas with anastomosed S-surface lineaments. These structures are truncated by traces of faults or fractures with NNE-SSW and ESE-WNW directions, which are more evident in the highest mountain ranges. The northern domain is characterized by reliefs of mountainous escarpments (AIT = 25° to 90°) and plateaus/tepui (i.e., flat top elevated sites with sub-vertical borders), both associated with sedimentary successions. In the southern portion of this domain, the sedimentary successions present beddings with an E-W direction and gentle dip to the north. Lineaments following the NNE-SSW and ESE-WNW directions represent brittle structures (faults and fractures).

The structural and geological maps were the products of integrating photo interpreted data (lineaments and homologous domains) and previous geological data (Figure 4). The regional basement (southern and central domains) includes the metavolcanic successions (Surumu Group and Cachoeira da Ilha Formation) and intrusive granitoid bodies (Pedra Pintada and Aricamã suites), whose gamma spectrometric response respectively corresponds to warm and light tones (Figure 3B). Northward, the volcano-sedimentary successions of the Roraima Supergroup cover this volcano-plutonic basement. To the south, quaternary unconsolidated sedimentary covers (Boa Vista and Areias Brancas formations, detrital-lateritic covers, and alluvial deposits) predominate in the flattened landscape, with inselbergs and higher reliefs exposing locally the basement inliers (Figure 3E).

The spatial analysis of the structures and the rosette diagrams allow the definition of two structural patterns. One of them is essentially ductile-brittle and occurs mainly in the metavolcanic successions. The metavolcanic layers are folded and affected by shear zones that, together with the axial plane solid-state foliation (S-surface lineaments and magnetic web), follow a WNW-ESE-trending direction (Figure 5A, 5B, and 5C). The second structural pattern stands out in the granitoid bodies and sedimentary rocks of the northwest portion, represents brittle structures (e.g., faults, fractures, and mafic dikes) and follows the NNW and NNE directions (Figure 5D and 5E).

4.2 Deformation patterns: field remote observations and structural data

The physiographic features supported by the Surumu Group volcanic succession reveals a series of folds with limbs plunging north and south, in agreement with the previously photo interpreted structural pattern. These chevron folds are gentle to open, parallel, and asymmetrical (Figure 6A). There are also "M" folds in the antiformal hinge zones (Figure 6B). The southern border of the Arai Formation presents parallel-trending structures, albeit with different styles. The folds are gentle and with rounded hinges (Figure 6C). Fault-bend folds are related to deformation over duplex fronts. A sub-horizontal thrust fault in the Lilás Range (see Figure 4A) indicates northward mass transport (Figure 6D). Another northward bending tighter folds can be related to covered thrust fronts. Following the northern direction into the Pacaraima Block (Reis et al. 2017; see Figure 1B), in the Arai Formation, the folds are increasingly gentle, and the layers show a low-angle dip to the north.

The volcanic rocks (Surumu Group and Cachoeira da Ilha Formation) present a pervasive solid-state foliation that follows an E-W direction with a sub-vertical southward dip (Figures 7A and 7B). However, a northward dipping foliation predominates in the southwest side of the belt (e.g., near Surumu Village; see Figure 4A). This secondary foliation is less penetrative in the coherent metavolcanic rocks. The mineral stretching lineations are mostly down-dip, with some oblique lineation plunging to the southwest. The bedding attitude tends to follow the same direction of the foliation but with low to moderate dip-angle, sub-horizontal in the hinge areas (Figure 9A). The volcanic layers show disharmonic open folds, with hinges ranging from angular to rounded and axial plane parallel to the solid-state foliation (Figure 7C), but parasitic folds are rare. There is an alternation of rheologically distinct thin layers within this succession (Figure 7D). Quartz veins of centimetric to metric thickness follow the foliation trend.

The (conglomeratic) sandstones of Arai Formation present a sparse secondary foliation (deformation partition) with nearly east-west direction with a steep southward dip parallel to the foliation observed in the basement rocks (Figures 7E, 7F, and 9B). Back-thrusts observed in the outcrop scale are present (Figure 7G). Centimetric quartz veins are lodged parallel to the bedding or filling fractures. This structural framework is limited to the lower portion (or southern edge) of Arai Formation. However, the sedimentary layers of the rest of the formation are not folded, presenting only a northward gently dipping bedding.

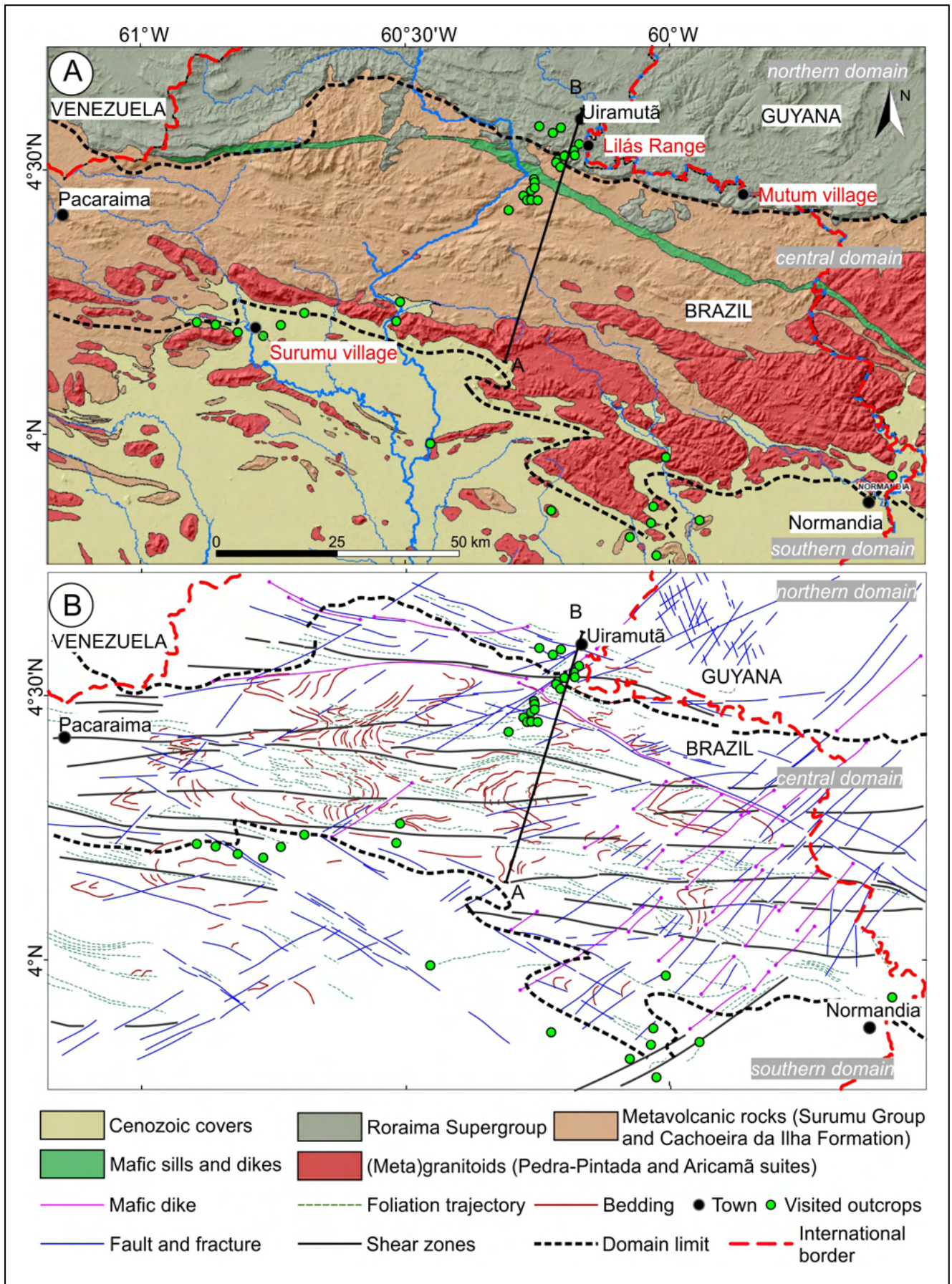


FIGURE 4. Geological and structural maps of the study area. (A) Interpretive geological map with a domain-based subdivision. (B) Structural map exhibiting the lineaments and corresponding geological interpretations. The green points correspond to the visited outcrops in this paper. Some key localities are highlighted in red letters in Figure 4A.

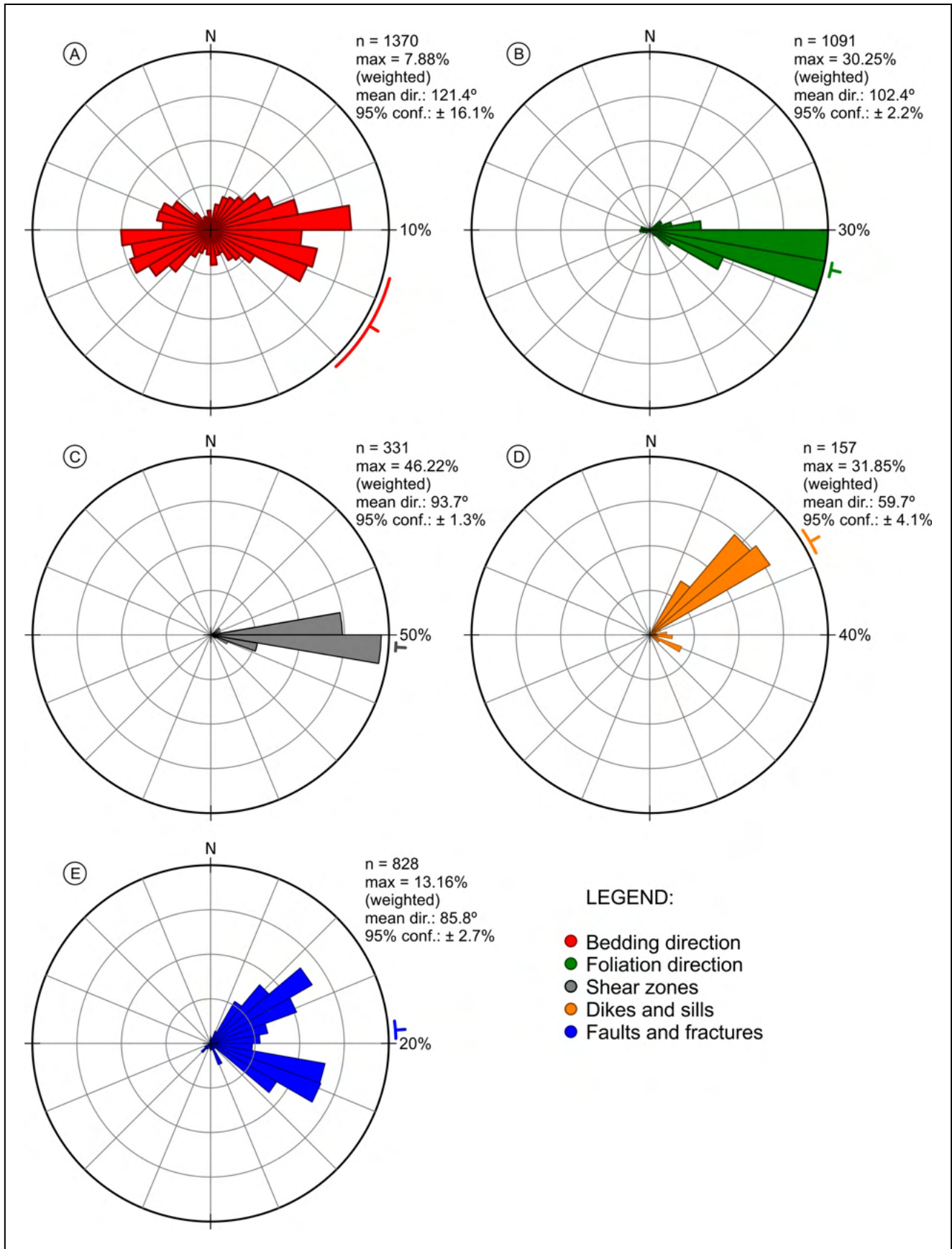


FIGURE 5. Rose diagrams of structural lineaments of Figure 4B. Lineaments related to: (A) bedding direction, (B) solid-state foliation direction, (C) shear zones, (D) dike and sill directions, and (E) faults and fractures.

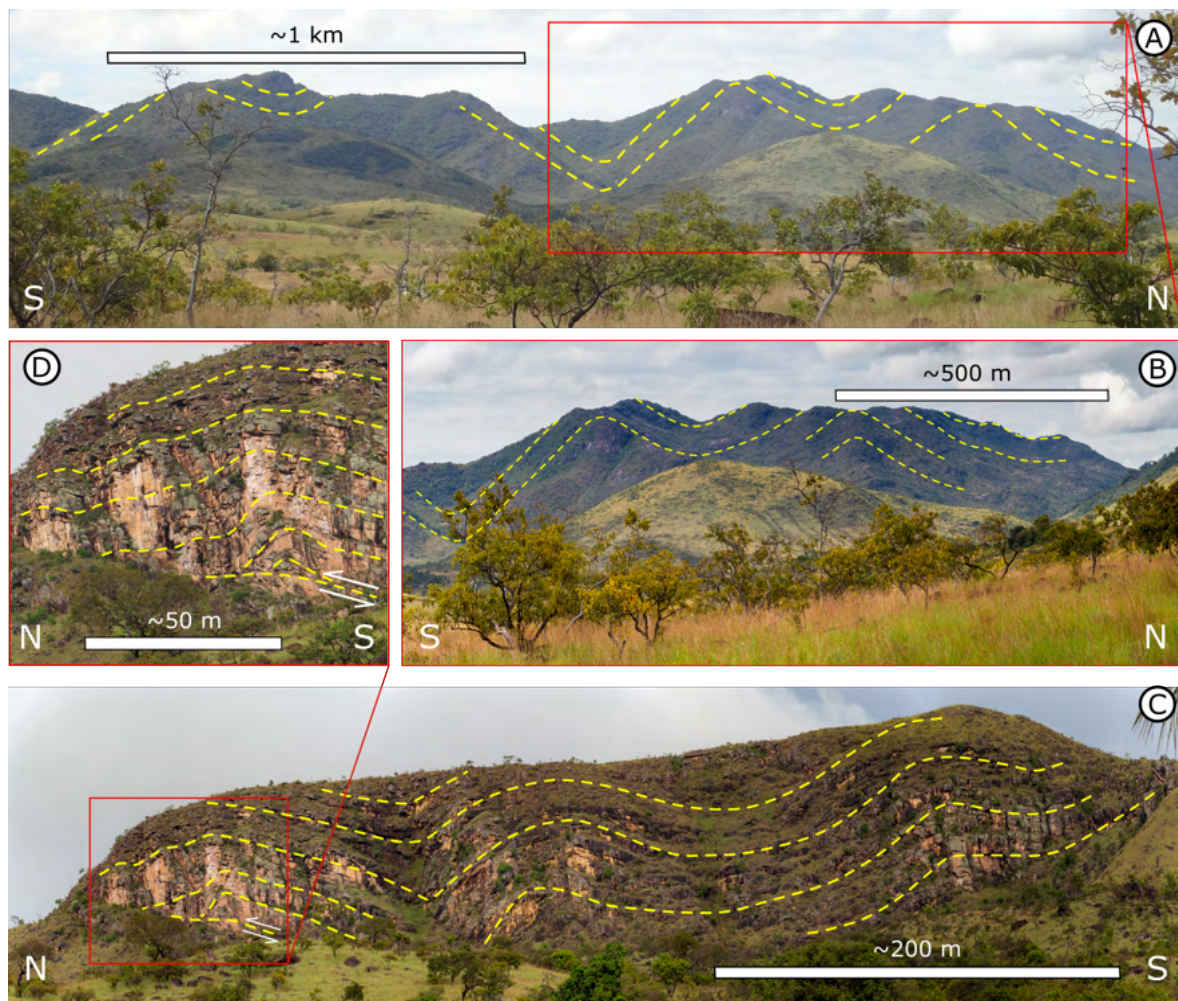


FIGURE 6. Geomorphological features and structural patterns of the Surumu and Arai successions. Observations along the BR-171 road. (A) Open chevron folds with sub-horizontal axes affecting volcanic layers of the Surumu Group. (B) A closer view of "M" folds in a hinge zone where it is possible to correlate anticlines to the highest points of the hills. (C) West view of Lilás Range, located in the southern border of Arai Formation and near Uiramutã city, revealing open, gentle folds with sub-horizontal axes in sandstone layers. (D) Closer view of Lilás Range where a fault-bend fold was formed over a thrust duplex, indicating mass transport to the north.

The Pedra Pintada and Aricamã (meta)granitoids, located in the southern portion of the belt, usually display a discrete to locally pronounced E-W-trending sub-vertical foliation (Figure 8A), although they preserve some primary features (e.g., subhedral phenocrysts and enclaves following the flow structure). The solid-state foliation is not penetrative in the granitoids, more pronounced at the edge of the outcropping bodies. Shear zones affect the border of the granitoid bodies (Figure 8B). Quartz veins of metric thickness follow the NNE-SSW-trending lineaments associated with brittle structures (Figure 9C).

4.3 Microstructural analysis

The felsic-intermediate metatuffs (Surumu Group) present porphyritic texture with a very fine-grained to a cryptocrystalline quartz-feldspathic matrix (<50 micrometers), besides subhedral plagioclase and subordinate quartz phenocrysts, and lithic and pumice fragments. Biotite is the main iron-magnesium mineral and occurs in the matrix and as phenocrysts. Zircon, pyrite, and apatite comprise the accessory phases. The plagioclase phenocrysts present

secondary epidote and sericite inclusions. Variations in granulation, phenocryst proportion, and composition evidence the primary planar structure (Sb; Figure 10A). Sericite, chlorite, and actinolite-tremolite are the metamorphic phases, while carbonate and epidote are alteration products. These secondary phases occur in the matrix, defining the solid-state foliation and filling microbands and pressure shadow (Sf; Figure 10). Quartz aggregates make up most of the foliated matrix, presenting strong undulatory extinction, recrystallization, and sub-grain rotation, which indicate considerable crystal-plastic deformation.

The quartz phenocrysts exhibit crystal-plastic deformational features (e.g., stretching, undulatory extinction, recrystallization, and sub-grain rotation). However, the plagioclase phenocrysts present brittle deformational features as fractures, slices dislocated in "en echelon" pattern, and crystal fragments incorporated into the foliated matrix (Figures 10E and 10F). The plagioclase phenocrysts act as porphyroclasts, with pressure shadows filled by quartz, calcite, biotite, and muscovite (Figures 10B and 10C). In sites with a substantial quantity of phenocrysts and lithic fragments, the secondary foliation deflects, forming anastomosed surfaces, and the pressure shadows are the primary indicator of

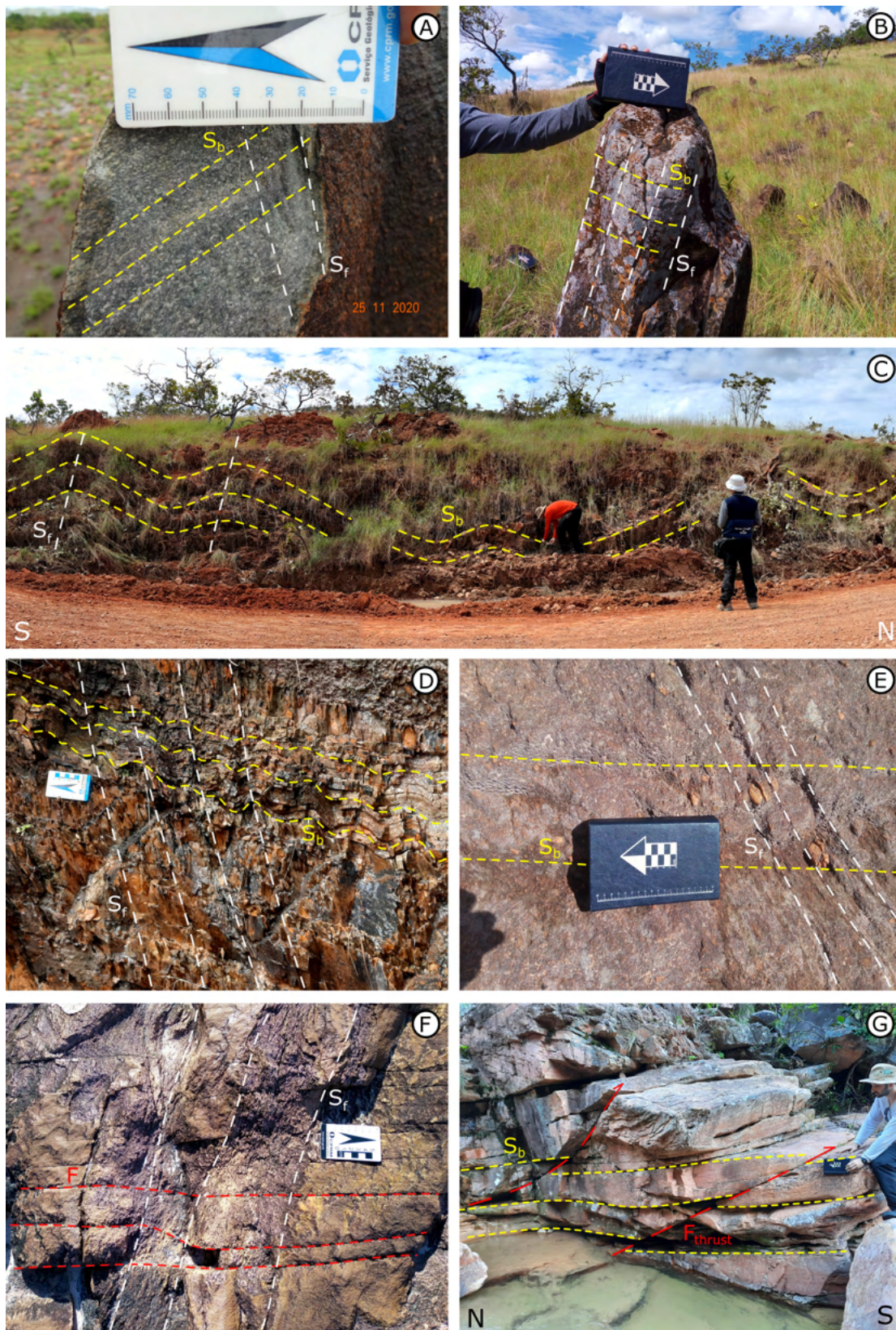


FIGURE 7. Geological structures in outcrops of the Surumu Group and Arai Formation. (A and B) Metatuff of the Surumu Group with a southward steeply dipping solid-state foliation (S_f) crossing the northward dipping bedding (S_b). (C) Roadcut outcrop, beside the road BR-171, revealing open folds with a southward steeply dipping axial plane parallel to the solid-state foliation; and (D) parasitic open folds affecting volcaniclastic layers of the Surumu Group. (E) Conglomeratic sandstone sapolite (Arai Formation) outcropping in a roadcut beside the road BR-171, presenting a southward steeply dipping cleavage; the cleavage intercepted and cracked the quartz pebbles. (F) Horizontal sandstone pavement of Arai Formation exhibiting N-S fractures and deformation partitioning of the E-W-trending foliation. (G) Northward dipping back-thrusts affecting sandstone layers of Arai Formation near the Paiuá Waterfall. The arrows on the scales indicate the north direction.



FIGURE 8. Geological structures in outcrops of Aricamã and Pedra Pintada suites. (A) Solid-state south-dipping foliation in metagranitoid of Aricamã Suite. (B) ESE-WNW-trending solid-state foliation in shear zone crossing metagranitoid of Pedra Pintada Suite. The arrows on the scales indicate the north direction.

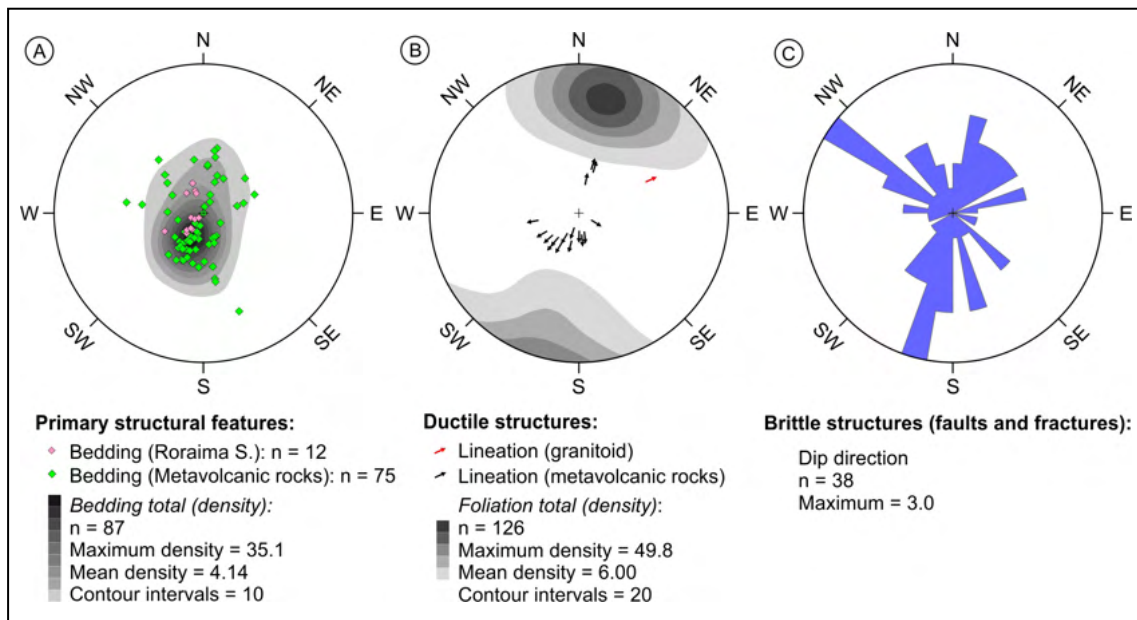


FIGURE 9. Lower hemisphere equal area stereograms with the structural data of the northeastern region of Roraima state (north-central Guiana Shield), related to the (A) primary structural features and secondary (B) ductile and (C) brittle structural features. Roraima S.: Roraima Supergroup.

the dextral kinematics (Figures 10D, 10E, and 10F). Locally, non-penetrative cleavage planes (S_c) may be present.

The (meta)granitoids of the region (i.e., Aricamã and Pedra Pintada suites) often show graphic texture, suggesting shallow-crustal level emplacement (Figure 11A). Samples collected in the border of these granitoid exposures present shear zones with thicknesses ranging from decimeters to millimeters. Grain-size reduction and development of S-C and S-C-C' microstructures in these spatial-limited zones (Figures 11B, 11C, and 11D) indicate dynamic metamorphism and dextral and sinistral kinematics are observed. The fabric of the sandstone basal layers of Arai Formation present undulatory extinction, microcracks, and sub-grain rotation as intragranular microstructural features (Figure 11E). The contact among the quartz grains ranges from interlobate to serrated and present bulging recrystallization texture. The matrix occupies the few spaces remaining among the quartz grains and comprises secondary sericite (Figure 11F).

5 Discussion

5.1 Structural framework: geometry, rheological control, and kinematics

The multi-scale structural dataset of the northeastern Roraima state (north-central Guiana Shield) displays a consistent fractal pattern. The photo interpreted bedding lineaments in the central domain, where the metavolcanic succession are dominant (Figure 4), present the first-order folds with kilometric wavelength and hinge lines with near east-west-trending direction. Similarly, the second-order folds stand out in the landscape while, at the outcrop scale, the third- and fourth-order folds appear (Figure 6A, 6B, 7C, and 7D). The south-plunging limbs tend to be longer than the north-plunging limbs, indicating northward mass transport.

The morphological variation of the folding patterns is mostly associated with differential rheology within layers and

variations of thickness, reflecting the competence contrast and crustal level in which the rocks were deformed. The metavolcanic rocks of the central domain show alternating compositional layers at a shallow crustal level, and it defines gentle to open chevron folds. Stratigraphically above (northern domain), the thick sandstone layers of Arai Formation show gentle folds and close to tight fault-bend folds above sub-horizontal thrust faults fronts (Figure 12). Similarly to the folds in the metavolcanic succession, the

south-dipping limbs in Arai Formation tend to be longer than the north-dipping ones.

On the regional scale, the photo interpreted secondary foliation is ubiquitous in the metavolcanic successions and follows an E-W- to ESE-WNW-trending direction (mean direction: $102.4^\circ \pm 2.2^\circ$), matching with the hinge lines direction of the megafolds (Figures 4 and 5). The same pattern observed in the physiography occurs in outcrop-scale parasitic folds, where the folds show south and north

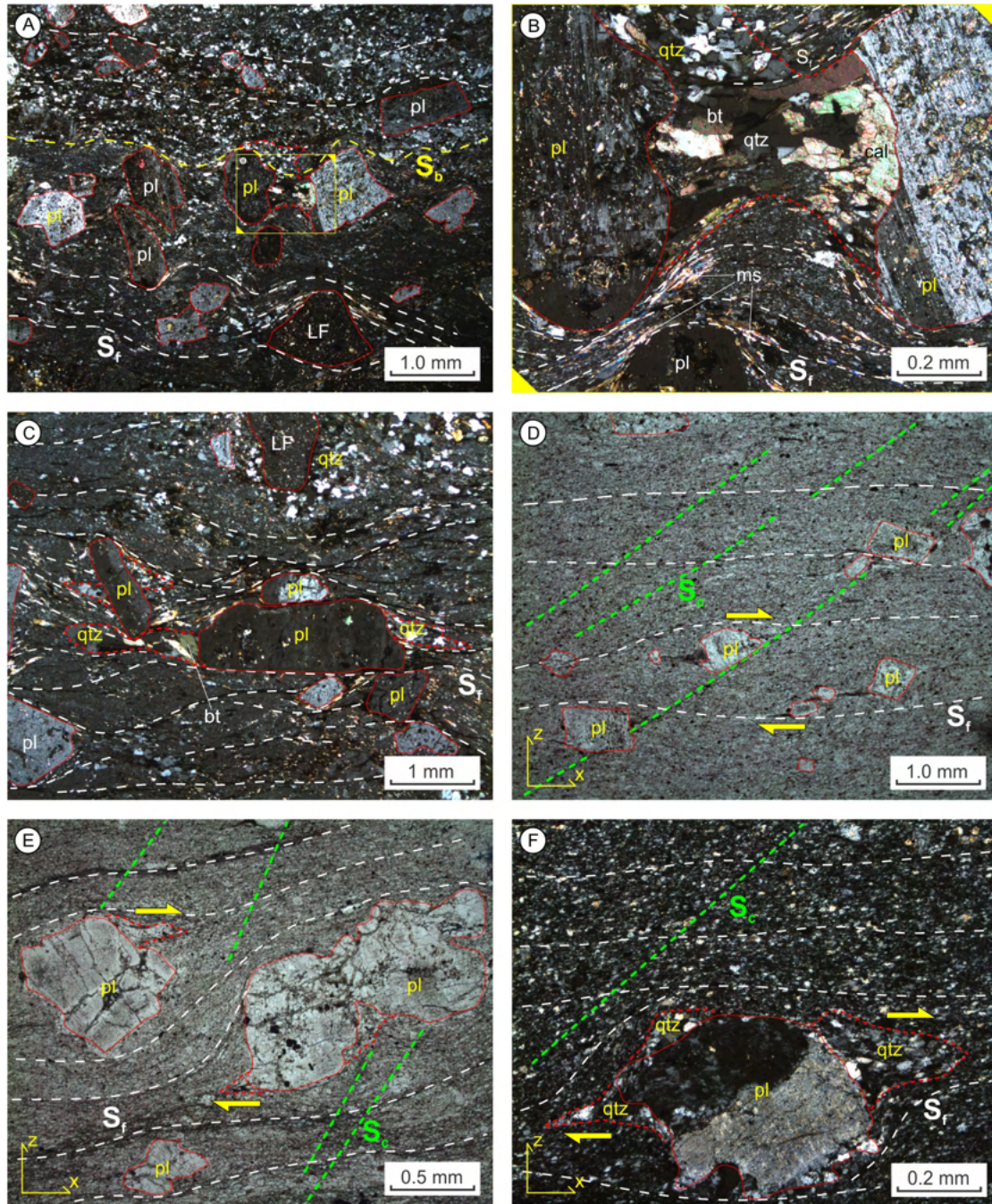


FIGURE 10. Microstructural features of the Surumu Group metavolcanic rocks. (A) Metatuff with bedding (S_b) sub-parallel to the solid-state foliation (S_f) embracing phenocrysts and lytic fragments, and (B) zoom in the pressure shadow among the plagioclase phenocrysts. (C) Anastomosed solid-state foliation dodging from phenocrysts in a metatuff. (D) Oriented metatuff sample with penetrative solid-state foliation and spaced cleavage planes (S_c) being affected by dextral shearing, in which (E) fractured plagioclase phenocrysts are the main kinematic indicators as indicated by (F) quartz-filled pressure shadows. Mineral abbreviations: pl = plagioclase; qtz = quartz; ms = muscovite; bt = biotite; cal = calcite. Red dashed lines bound the shadow pressure zones.

dipping limbs with a steep south-dipping foliation, parallel to the axial plane (Figures 6, 7, and 9). In the southeastern portion of the study area, this foliation tends to dip northward. The mineral stretching lineation in these planes varies from down-dip to slightly oblique plunging to the southwest (Figure 9). The recognition of deformational foliation at the micro-scale confirms its penetrative and ubiquitous character in the metatuffs. However, the deformational foliation is less intense in the coherent metavolcanic rocks.

The basal sandstones at the bottom of Arai Formation do not present ubiquitous solid-state foliation. Due to

deformation partitioning in an upper crustal level, the foliation is characterized by a spaced cleavage and follows the same regional E-W- to ESE-WNW-trending direction. This foliation is parallel to the axial plane of gentle folds. The gently southward-dipping thrust fault in the southern portion of the Arai Formation (Figure 12) is coherent with the kinematics seen in the metavolcanic basement. The outcrop-scale north-dipping thrust faults show minor offsets (Figure 7G) and represent back-thrusts.

The granitoids presented distinct behavior during the tectonic stress. Due to its intrinsic rheological competence,

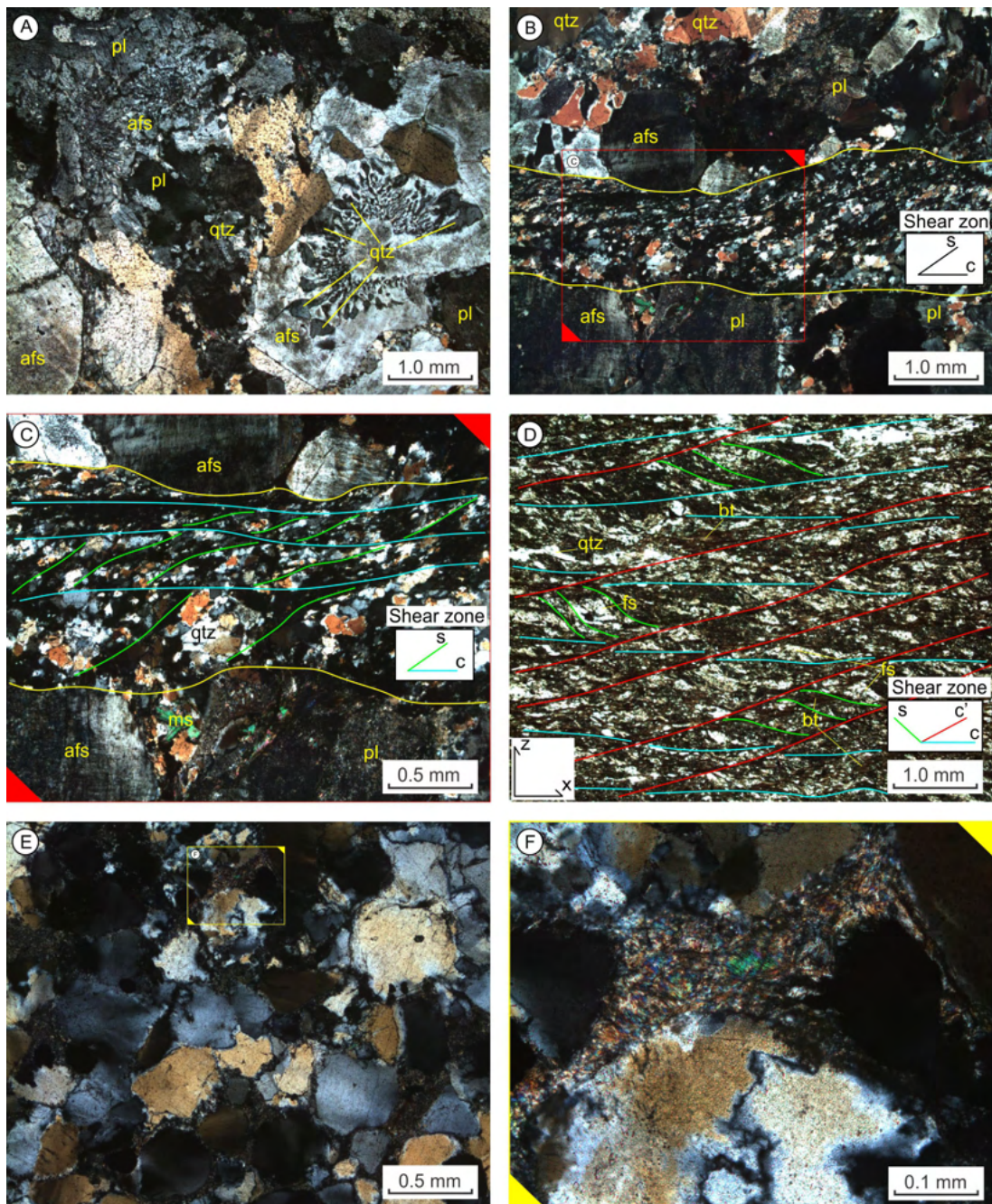


FIGURE 11. Microstructural features of the shallow granitoids of the Orocaima Igneous Belt and Arai Formation sandstones. (A) Metasyenogranite with graphic texture and (B and C) micro shear zone. (D) Oriented sample of altered mylonite presenting S-C-C' structure. (E) Sandstone with quartz grains presenting undulatory extinction, sub-grain rotation, and interlobate border, (F) highlighting sericite formation in the matrix. Mineral abbreviations: pl = plagioclase; afs = alkali feldspar; qtz = quartz; ms = muscovite; bt = biotite; fs = feldspar. Yellow lines bound the shear zones in photomicrographs B and C.

the folding process does not affect these plutonic rocks like seen in volcanic successions. Deformation concentrates in the granitoids' border. The structural lineaments (Figure 4B) match with the E-W-trending mylonitic foliation (Figure 8B), and the vertical component of the oblique to down-dip lineation in the bordering shear zones indicates a tectonic transport from lower to higher crustal levels. Also, considering the original relation of the volcano-plutonic system – chrono correlated volcanic rocks over the magmatic chambers – the contrasting current situation should be analyzed. The (meta)granitoids reach higher topographic altitudes than the metavolcanic succession and, besides, the near ESE-WNW-trending extremely elongated shape in the map (Figure 4) may not resemble the intrusive bodies original morphology. These factors indicate that the outcropping plutonic rocks correspond to tectonic slices of the shallow basement involved in the deformational event. Considering the involvement of the granitoids in the deformation and the tectonic inversion, it is interpreted that the southern domain presents thick-skinned tectonics, while thin-skinned tectonics predominates northward (central and northern domains; Figure 4).

The deformational features of the quartzofeldspathic metavolcanic rocks indicate metamorphic conditions compatible with greenschist to epidote-amphibolite facies. This is evident in the microstructural features. The quartz grains present ductile deformational features (e.g., stretching, recrystallization, and sub-grain rotation) while the feldspar grains show brittle deformation (e.g., fracture). The regional pattern indicates heterogeneous metamorphism and deformation due to the development of E-W- to ESE-WNW- trending shear zones (Figure 4). In these zones, low- and medium-temperature mylonites (250-500°C; Trouw et al. 2009) were generated, sometimes breaking the short limbs of first- and second-order folds parallel to the axial plane and the secondary foliation. The microstructural features characterize brittle-ductile transitional conditions, in which the quartzo-feldspathic matrix presents feldspar phenocrysts with fractures besides discrete crystal-plastic recrystallization of the phenocrysts fragments (Figure 10). Sericite sheets are also common in low-pressure zones between boudinated porphyroclasts and waving films of refractory dissolution phases (Fe-oxides and biotite). Another characteristic of low- and medium-temperature

mylonites observed in these rocks is the abundance of asymmetric structures, which indicate dextral transpressive kinematics to this fold-and-thrust belt.

The upper conglomeratic sandstones (Arai Formation) present non-ubiquitous brittle deformational features. These sandstones developed low-temperature microstructures in quartz grains (i.e., undulatory extinction, microcracks, and sub-grain rotation). The deformation is conditioned by the rheology of the competent psamo-psefitic layers, manifesting as brittle compressional structures in an upper crustal level, like thrust faults (Figures 6D and 7G) and fractures in quartz pebbles parallel to the cleavage (Figure 7E). On the Tepequém Formation, directly correlated to Arai Formation (both basal successions of the Roraima Supergroup), Luzardo (2006) relates prehnite-pumpellyite metamorphic facies conditions, defined by the presence of pyrophyllite and illite/muscovite in deformed pelitic rocks that assigned temperatures below 400°C.

5.2 Tectonic scenario of the north-central Guiana Shield

Previous studies (Pinheiro et al. 1990; Fraga et al. 1994a, 1994b, 2010; Luzardo 2006; Fernandes Filho et al. 2012; Fraga et al. 2017b) correlated the structural framework of the north-central Guiana Shield to the K'Mudku Event, which produces intense crustal reworking during the interval between 1.49-1.15 Ga. Nevertheless, the few geochronological data that may refer to this thermal event (1263 ± 47 to 721 ± 36 ; K-Ar analyses by Amaral 1974) are not constrained by the K'Mudku age interval. Considering the method limitations of the available K-Ar whole-rock data, more comprehensive and modern petrochronological studies are necessary to unravel the tectonic history of the area.

According to geophysical studies focusing on the central portion of the Guiana Shield (Costa 2005; Oliveira 2018; Oliveira et al. 2019), the NE-SW lineaments – usually related to the K'Mudku Event – overlaps E-W-trending lineaments correlated to deeper structures (Orosirian basement). The geophysical response reveals E-W-trending compressional structures and shear zones (first deformational event - D1) overlapped by NE-SW- to N-S-trending shear zones, faults, and fractures (second deformational event - D2). Thus, from

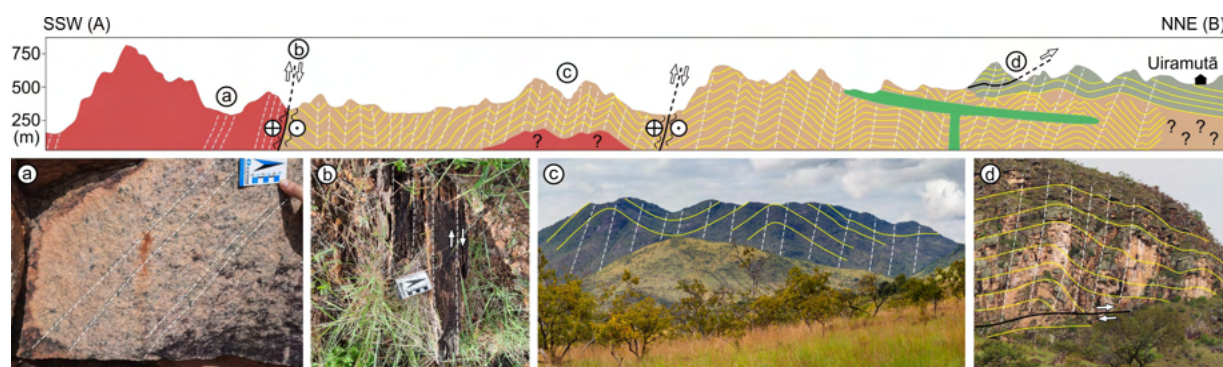


FIGURE 12. Schematic geological cross-section (A-B section in Figure 4) of the north-central Guiana Shield. The cross-section lengthens by 55 kilometers following a SSW-NNE-trending direction approximately orthogonal to the main trend of the fold-and-thrust belt. Yellow continuous line = bedding; white dashed line = secondary foliation; thick black line = fault. Below the cross-section, the principal structural features are: (a) Aricamã Suite granite with a south-plunging foliation; (b) mylonite with dextral kinematics in a granitoid; (c) open chevron folds affecting the metavolcanic rocks of the Surumu Group; and (d) gentle folds and low-angle thrust faults affecting sandstone layers of Arai Formation.

the geometric point of view, the framework of the fold-and-thrust belt studied in this work (E-W- to ESE-WNW trend direction; figures 4, 9 and 12) does not match with the K'Mudku tectonics, but with the Orosirian structures of the southward basement.

Geochronological data for the southern and central portions of the Roraima state present metamorphic records between 1.99 and 1.91 Ga. Costa (2005) assigned a 1.920 ± 2 Ma metamorphic age (U-Pb in titanite, biotite orthogneiss sample) to Rio Urubu Igneous Belt, besides Sm-Nd isotopic ages (garnet and whole-rock isochron) of 1.910 ± 45 Ma and 1910 ± 150 Ma to high-grade metasedimentary rocks (garnet gneisses) of Cauarane-Coerene Belt (Figure 1). Garcindo et al. (2018) also present a metamorphic age in 1.915 ± 12 Ma (U-Pb SHRIMP in zircon) of a high-grade metasedimentary rock of the Cauarane Group. Fraga et al. (2017c) present geochronological data (U-Pb SHRIMP in zircon) of a Cauarane Group's paragneiss sample in which low-Th/U ratios grains (<0.1) plot in the age intervals of 1990-1960 Ma and 1940-1920 Ma. However, Fraga et al. (2017c) interpret that the emplacement of large igneous bodies of Orocaima and Rio Urubu belt – in a post-tectonic setting – was the cause of these metamorphic records due to thermal perturbation, fluid input, and partial melting.

Some records of this Orosirian tectonics also occur southwards. Almeida et al. (2007) present a crystallization age of 1909 ± 9 Ma obtained in leucogranite lenses hosted by the Martins Pereira Suite orthogneiss (~ 1.97 Ga crystallization age). If these leucogranite lenses represented the leucosome, this magmatism could be related to the same event that affected the Cauarane-Coerene Belt. Similarly, Oliveira et al. (2019) assigned a metamorphic age of 1921 ± 27 Ma to another rock of the Martins Pereira Suite located further north. Rodrigues and Macambira (2021) also present a crystallization age of 1913 ± 29 Ma referring to a metagranite sample of Rio Urubu Igneous Belt. In a western metasedimentary succession (Aracá Formation – Amazonas state), Santos et al. (2003) assigned a detrital zircon population with 1915 ± 8 Ma to record a relevant tectonic event in the source area.

The correlation of the Middle Orosirian metamorphic event recorded in the central Guiana Shield with the structures described in this study is indeed corroborated by the nearly E-W-trending lineaments, which is associated with 1.91 Ga sheet-like leucogranites in Martins Pereira Suite (Almeida et al. 2007) and NW-SE- to E-W-trending metamorphic foliation in Cauarane-Coerene Belt (Garcindo et al. 2018). This interpretation is also in agreement with the observations of a WNW-ESE to NW-SE structural trend (Orosirian basement structures) later reworked by the NE-SW structures (K'Mudku Intracontinental Orogeny) at the central Guiana Shield (Oliveira et al. 2019). In the study area, the late NE-SW lineaments host Mesozoic dykes related to the processes of the Atlantic opening (Figure 4B).

Furthermore, the northwestern Roraima state (Parima region) may be pivotal to the Orosirian tectonics of the central Guiana Shield. Almeida et al. (2001) define several granitic associations intruding the Early Orosirian basement, including the S-type granites of Rio Couto Magalhães Suite, whose age remains unknown but can be associated with syn-tectonic magmatism in this crustal portion. However, this region still needs more data to elucidate its role in the regional tectonics.

6. Conclusions

A multi-scale approach to the structural framework of the north-central Guiana Shield reveals a consistent fractal pattern (i.e., satellite image, landscape, outcrop, and micro scales). The structural parallelism of different features suggests a common deformational path between the metavolcanic/plutonic basement (Orocaima Igneous Belt) and the Arai Formation metasedimentary layers. Their geometry reflects the rheological response to a compressional tectonics with mass transport to the north in a Proterozoic (unconstrained age) fold-and-thrust belt. Some conclusions and considerations are highlighted herein:

1. The satellite and aerogeophysical images offer some clues about a compressional setting, which could be related to a tectonic inversion that uplifted the shallow-granitoid slices (Aricamã and Pedra Pintada suites) over the supracrustal successions. E-W-trending anastomosed lineaments, also observed in the southward high-grade rocks of the Cauarane-Coerene, Rio Urubu belts, and Northern Uatumã-Anauá Domain (Martins Pereira Suite) are the main ductile-brittle structural pattern. This pattern was overprinted by the NNE-SSW- and ESE-WNW-trending lineaments correlated to brittle structural features.
2. The field data are in agreement with the interpretation of the remote sensing images. The E-W-trending lineaments correspond to the fold axial planes and the related secondary foliation in open to gentle folds in the Orocaima Igneous belt's volcanic rocks. The Arai Formation and shallow granitoids have the same orientation, although with a distinct degree. The secondary foliation presents a steep southward-dipping and contains high-rake mineral stretching lineations, although, at the southwestern portion, the foliation shows a southward vergence. The brittle structures (i.e., fractures and faults) correlate to the NNE-SSW- and ESE-WNW-trending straight lineaments.
3. Due to the relative competence, the secondary foliation is more penetrative in the volcanoclastic rocks. This foliation is spaced or discrete in more competent granitoids, sandstones, and coherent volcanic rocks. Nevertheless, their origins are both tectonic.
4. Most rocks present a southward dipping solid-state foliation with down-dip lineation, which suggests a frontal compressional setting. Some outcrops exhibit dextral shear zones with oblique lineations, indicating local lateral kinematic component. Further detailed structural mapping must reveal the role of the major structures controlling compressional and lateral movements.
5. Although previous studies relate the deformational features of the north-central Guiana Shield to the K'Mudku Event (1.49-1.15 Ga), the geometrical relations described in this study point out to earlier structures. The Cauarane-Coerene, Rio Urubu, Martins Pereira, and Orocaima belts present a consistent E-W- to ESE-WNW-trending structural framework – parallel to the fold-and-thrust belt described here – that can be correlated with a metamorphic event dated around 1.92-1.91 Ga. Indeed, petrochronological constraints must be applied to test this hypothesis.

Acknowledgements

This paper is a contribution from the Geological Survey of Brazil, through the "Geologia e Recursos Minerais do

Estado de Roraima” project (Geology and Mineral Resources of the Roraima state) with the partnership of professors of the Geology Department of the UFMG. The first structural observations that promoted this work were made in a field trip with the researcher Paulo Roberto Rodrigues Benevides, and we are grateful for the opportunity and partnership of this inspiring field trip. We are thankful to the Uiramutã and Normandia population and the local Macuxi communities that allow the field trip and sample collecting. We are grateful for the support and contributions of the JGSB editorial board and the anonymous reviewers for constructive comments and suggestions that substantially improved the manuscript.

Authorship credits

Author	A	B	C	D	E	F
TAAM						
ACSO						
MEA						
FAC						
TAN						

A - Study design/Conceptualization B - Investigation/Data acquisition
 C - Data Interpretation/ Validation D - Writing
 E - Review/Editing F - Supervision/Project administration

References

- Almeida M.E., Fraga L.M.B., Macambira M.J.B. 1997. New geochronological data of calc-alkaline granitoids of Roraima State, Brazil. In: South-American Symposium on Isotope Geology, Brazil, 1, 34-37.
- Almeida M.E., Ferreira A.L., Pinheiro S.S. 2001. Principais associações graníticas do oeste do estado de Roraima. In: Simpósio de Geologia da Amazônia, 7, 878-881. Available online at: <http://arquivos.sbg-no.org.br/BASES/Anais%207%20Simp%20Geol%20Amaz%20Nov-2001-Belem.pdf> / (accessed on 06 January 2022).
- Almeida M.E., Macambira M.J.B., Oliveira E.C. 2007. Geochemistry and zircon geochronology of the I-type high-K calc-alkaline and S-type granitoid rocks from southeastern Roraima, Brazil: Orosirian collisional magmatism evidence (1.97–1.96 Ga) in central portion of Guyana Shield. *Precambrian Research*, 155(1-2), 69-97. <https://doi.org/10.1016/j.precamres.2007.01.004>.
- Amaral G. 1974. Geologia pré-cambriana da região amazônica. Habilitation Thesis, Universidade de São Paulo, São Paulo, 212 p. Available online at: <https://teses.usp.br/teses/disponiveis/livredocencia/44/tde-24062016-160651/en.php> / (accessed on 06 January 2022).
- Barbosa N.A. 2020. Vulcanismo orosiriano no norte de Roraima, Cráton Amazônico. MSc Dissertation, Instituto de Geociências, Universidade de Brasília, Brasília, 98 p. Available online at: <https://repositorio.unb.br/handle/10482/39224> / (accessed on 06 January 2022).
- Barbosa N.A., Fuck R.A., Souza V.S., Dantas E.L., Tavares Júnior S.S. 2021. Evidence of a Palaeoproterozoic SLIP, northern Amazonian Craton, Brazil. *Journal of South American Earth Sciences*, 111, 103453. <https://doi.org/10.1016/j.jsames.2021.103453>.
- Barron C.N. 1966. Notes on the stratigraphy of Guyana. In: Guiana Geological Conference, 7, Records Geological Survey, 6, 1-28.
- Bonfim L.F.C., Ramgrab G.E., Uchôa I.B., Medeiros J.B., Viegas Filho J.R., Mandetta P., Kuyumjian R.M., Pinheiro S.S. 1974. Projeto Roraima – Folhas NB.20-Z-B e NB.20-Z-D. Manaus, CPRM, 206 p. Available online at: <https://rigeo.cprm.gov.br/handle/doc/3692> / (accessed on 06 January 2022).
- Bryan S.E. 2007. Silicic Large Igneous Province. *Episodes*, 30(1), 20-31. <https://doi.org/10.18814/epiugs/2007/v30i1/004>.
- Bryan S.E., Ernst R.E. 2008. Revised definition of Large Igneous Provinces (LIPs). *Earth-Science Reviews*, 86(1-4), 175-202. <https://doi.org/10.1016/j.earscirev.2007.08.008>.
- Butler R.W.H., Bond C.E., Cooper M.A., Watkins H. 2018. Interpreting structural geometry in fold-thrust belts: why style matters. *Journal of Structural Geology*, 114, 251-273. <https://doi.org/10.1016/j.jsg.2018.06.019>.
- Cordani U.G., Teixeira W. 2007. Proterozoic accretionary belts in the Amazonian Craton. In: Hatcher R.D., Carlson M.P., McBride J.H., Martinez-Catalan J.R. 4-D Framework of Continental Crust. Boulder, Geological Society of America, p. 297-320. [https://doi.org/10.1130/2007.1200\(14\)](https://doi.org/10.1130/2007.1200(14)).
- Costa J.B.S., Reis N.J., Pinheiro S.S., Pessoa M.R. 1991. Organização litoestrutural do Proterozóico Médio do extremo norte do estado de Roraima. In: Simpósio de Geologia da Amazônia, 3, 179-192. Available online at: http://sbg.sitepessoal.com/anais_digitalizados/nucleonorte/Anais_3_Simp_Geol_Amaz_Dez-1991-Belem.pdf / (accessed on 07 January 2022).
- Costa J.A.V. 1999. Tectônica da região nordeste do estado de Roraima. PhD Thesis, Instituto de Geociências, Universidade Federal do Pará, Belém, 315p.
- Costa J.A.V., Costa J.B.S., Macambira M.J.B. 2001. Grupo Surumu e Suíte Intrusiva Saracura, RR - Novas Idades Pb-Pb em zircão e interpretação tectônica. In: Simpósio de Geologia da Amazônia, 7, 890-893. Available online at: arquivos.sbg-no.org.br/BASES/Anais_7_Simp_Geol_Amaz_Nov-2001-Belem.pdf / (accessed on 13 January 2022).
- Costa S.S. 2005. Delimitação do arcabouço tectônico do Cinturão Guiana Central, estado de Roraima, com base na análise integrada dos dados geofísicos, geológicos, isotópicos e imagens de satélite. PhD Thesis, Instituto de Geociências, Universidade Estadual de Campinas, Campinas, 188 p.
- Fernandes Filho L.A., Pinheiro R.V.L., Truckenbrodt W., Nogueira A.C.R. 2012. Deformação das rochas siliciclásticas paleoproterozoicas do Grupo Araí como exemplo das reativações de falhas do embasamento, Serra do Tepequém, Roraima, norte do Brasil. *Revista Brasileira de Geociências*, 42(4), 785-798. <https://doi.org/10.5327/Z0375-75362012000400010>.
- Fraga L.M.B., Reis N.J., Pinheiro S.S. 1994a. Arranjo estrutural do segmento sul do bloco Pacaraima - estado de Roraima. In: Simpósio de Geologia da Amazônia, 4, 7-9. Available online at: http://sbg.sitepessoal.com/anais_digitalizados/nucleonorte/Anais_4_Simp_Geol_Amaz_Junho-1994_Vol_1-Belem.pdf / (accessed on 07 January 2022).
- Fraga L.M.B., Reis N.J., Pinheiro S.S. 1994b. Serra Tepequém: uma estrutura relacionada à inversão da Bacia Roraima. In: Congresso Brasileiro de Geologia, 38, 2, 294-295. Available online at: <http://www.sbgeo.org.br/home/pages/44#AnaisCongressosBrasileirosdeGeologia> / (accessed on 07 January 2022).
- Fraga L.M.B., Reis N.J. 1996. A reativação do cinturão de cisalhamento Guiana Central durante o episódio K'Mudku. In: Congresso Brasileiro de Geologia, 39, 424-426. Available online at: <http://www.sbgeo.org.br/home/pages/44#AnaisCongressosBrasileirosdeGeologia> / (accessed on 07 January 2022).
- Fraga L.M.B., Haddad R.C., Reis N.J. 1997. Aspectos geoquímicos das rochas granitóides da suíte intrusiva Pedra Pintada, norte do estado de Roraima. *Revista Brasileira de Geociências*, 27(1), 3-12. <https://doi.org/10.25249/0375-7536.1997312>.
- Fraga L.M.B., Reis N.J., Dall'Agnol R., Armstrong R. 2008. Cauarane-Coeroene Belt – The tectonic southern limit of the preserved Rhyacian crustal domain in the Guyana Shield, northern Amazonian craton. In: International Geological Congress, 33.
- Fraga L.M.B., Reis N.J., Dall'Agnol R., Armstrong R. 2009. Cauarane-Coeroeni belt – the main tectonic feature of the central Guyana Shield, Northern Amazonian Craton. In: Simpósio de Geologia da Amazônia, 13, 142-145. Available online at: <https://rigeo.cprm.gov.br/handle/doc/896> / (accessed on 07 January 2022).
- Fraga L.M.B., Dreher A.M., Graziotin H.F., Reis N.J., Farias M.S.G., Ragatky D. 2010. Geologia e recursos minerais da folha Vila de Tepequém – NA.20-X-A-III estado de Roraima, escala 1:100.000. Manaus, CPRM, 182 p. Available online at: <https://rigeo.cprm.gov.br/handle/doc/10920> / (accessed on 10 January 2022).
- Fraga L.M.B., Cordani U.G., Reis N.J., Nadeau S., Maurer V.C. 2017a. U-Pb SHRIMP and LA-ICPMS new data for different A-type granites of the Oroaima Igneous Belt, Central Guyana Shield, northern Amazonian Craton. In: Simpósio de Geologia da Amazônia, 15, 482-485. Available online at: http://sbg.sitepessoal.com/anais_digitalizados/nucleonorte/Anais_15_Simp_Geol_Amaz_Set-2017-Belem.pdf / (accessed on 10 January 2022).
- Fraga L.M.B., Dreher A.M., Reis N.J., Bettiolo L.M., Scandolara J.E. 2017b. Geologia e recursos minerais da folha Ilha de Maracá - NA.20-X-A, estado de Roraima. Manaus, CPRM, 48 p. Available online at: <https://rigeo.cprm.gov.br/handle/doc/21205> / (accessed on 10 January 2022).
- Fraga L.M.B., Cordani U.G., Roeber E.D., Nadeau S., Maurer V.C. 2017c. U-Pb SHRIMP new data on the high-grade supracrustal rocks of

- the Cauarane-Coeroeni Belt - insights on the tectonic Eo-Orosirian evolution of the Guiana Shield. In: Simpósio de Geologia da Amazônia, 15, 486-490. Available online at: http://sbge.org.br/anais_digitalizados/nucleonorte/Anais_15_Simp_Geol_Amaz_Set-2017-Belem.pdf / (accessed on 10 January 2022).
- Fraga L.M.B., Cordani U.G., Reis N.J., Dreher A.M., Kroonenberg S., Roeber E.D., Nadeau S. 2018. Rhyacian to Early Orosirian tectonic evolution of the Guyana Shield, northern Amazonian Craton. In: Congresso Brasileiro de Geologia, 49. Available online at: <http://cbg2018anais.siteoficial.ws/resumos/8851.pdf> / (accessed on 10 March 2021).
- Garcindo L.B., Queiroz L., Souza A.G.H., Lisboa T.M. 2018. Geologia da folha Rio Uraricoera (NA-20-X-B-IV), com ênfase no metamorfismo e geocronologia do Grupo Cauarane - NW de Boa Vista (RR). Congresso Brasileiro de Geologia, 49. Available online at: <http://cbg2018anais.siteoficial.ws/anexos/anais49cbg.pdf> / (accessed on 10 March 2021).
- Guy H. 1966. Quelques principes et quelques expériences sur la méthodologie de la photo-interprétation. In: International Symposium on Photo-interpretation, 2, 21-41.
- Ibanez-Mejia M., Ruiz J., Valencia V.A., Cardona A., Gehrels G.E., Mora A.R. 2011. The Putumayo Orogen of Amazonia and its implications for Rodinia reconstructions: new U-Pb geochronological insights into the Proterozoic tectonic evolution of northwestern South America. *Precambrian Research*, 191(1-2), 58-77. <https://doi.org/10.1016/j.precamres.2011.09.005>.
- Jacobsen B.H. 1987. A case for upward continuation as a standard separation filter for potential-field maps. *Geophysics*, 52(8), 1138-1148. <https://doi.org/10.1190/1.1442378>.
- Jessell M.W., Valenta, R.K. 1996. Structural geophysics: integrated structural and geophysical modelling. *Computer Methods in the Geosciences*, 15, 303-324. [https://doi.org/10.1016/S1874-561X\(96\)80027-7](https://doi.org/10.1016/S1874-561X(96)80027-7).
- Klein E.L., Almeida M.E., Rosa-Costa L.T. 2012. The 1.89-1.87 Ga Uatumã Silicic Large Igneous Province, northern South America. *LIP Commission*, 14 p. Available online at: <http://www.largeigneousprovinces.org/12nov/> / (accessed on 28 August 2020).
- Luzardo R. 2006. O metamorfismo da Serra do Tepequém (estado de Roraima). MSc Dissertation, Instituto de Ciências Exatas, Universidade Federal do Amazonas, Manaus, 77 p. Available online at: <https://tede.ufam.edu.br/handle/tede/3287> / (accessed on 10 January 2022).
- McQuarrie N., Ehlers T.A. 2017. Techniques for understanding fold-and-thrust belt kinematics and thermal evolution. *Geological Society of America Memoir*, 213, 25-54. [https://doi.org/10.1130/2017.1213\(02\)](https://doi.org/10.1130/2017.1213(02)).
- Oliveira A.C.S., Goulart L.E.A., Lopes P.R.S., Almeida M.E., Costa I.S.L., Rodrigues J.B. 2019. Orogenia Intracontinental K'Mudku: estudo estrutural, geofísico e geocronológico da faixa Granulítica Baraúana, Escudo das Guianas, região central de Roraima. In: Simpósio de Geologia da Amazônia, 16, 358-363. Available online at: http://sbge.org.br/anais_digitalizados/simposioamazonas/ANAIS_16_Simposio_Geologia_da_Amazonia.pdf / (accessed on 10 January 2022).
- Oliveira R.G. 2008. Arcabouço geofísico, isostasia e causas do magmatismo cenozoico da Província Borborema e de sua margem continental (nordeste do Brasil). PhD Thesis, Centro de Ciências Exatas da Terra, Universidade Federal do Rio Grande do Norte, Natal, 411 p. Available online at: <https://repositorio.ufrn.br/handle/123456789/18344> / (accessed on 10 January 2022).
- Oliveira V.S. 2018. Interpretação geofísico-geológica de uma porção setentrional do Cráton Amazônico. MSc Dissertation, Departamento de Geologia, Universidade Federal do Paraná, Curitiba, 115 p. Available online at: <https://hdl.handle.net/1884/58104> / (accessed on 10 January 2022).
- Pinheiro S.S., Reis N.J., Costi H.T. 1990. Geologia da região de Caburái, nordeste de Roraima. Escala 1:100.000. Programa Levantamentos Geológicos Básicos do Brasil, Manaus, DNPM, CPRM, 91 p. Available online at: <https://rigeo.cprm.gov.br/handle/doc/8386> / (accessed on 10 January 2022).
- Poblet J., Lisle R. 2011. Kinematic evolution and structural styles of Fold-and-Thrust Belts. *Geological Society, Special Publications*, London, 349(1), 1-24. <https://doi.org/10.1144/SP349.1>.
- Reis N.J., Teixeira W., Hamilton M.A., Bispo-Santos F., Almeida M.E., D'Agrella-Filho M.S. 2013. Avanço mafico magmatism, a late Paleoproterozoic LIP in the Guiana Shield, Amazonian Craton: U-Pb ID-TIMS baddeleyite, geochemical and paleomagnetic evidence. *Lithos*, 174(1), 175-195. <https://doi.org/10.1016/j.lithos.2012.10.014>.
- Reis N.J., Nadeau S., Fraga L.M.B., Bettiello L.M., Faraco M.T.L., Reece J., Lachhman D., Ault R. 2017. Stratigraphy of the Roraima supergroup along the Brazil Guyana border in the Guiana shield, Northern Amazonian Craton - results of the Brazil Guyana Geology and Geodiversity Mapping Project. *Brazilian Journal of Geology*, 47(1), 43-57. <https://doi.org/10.1590/2317-4889201720160139>.
- Reis N.J., Cordani U., Goulart L.E.A., Almeida M.E., Oliveira V., Maurer V.C., Wahfried I. 2021a. Zircon U-Pb SHRIMP ages of the Demêni-Mocidade Domain, Roraima, southern Guyana Shield, Brazil: extension of the Uatumã Silicic Large Igneous Province. *Journal of the Geological Survey of Brazil*, 4(1), 61-76. <https://doi.org/10.29396/jgsb.2021.v4.n1.4>.
- Reis N.J., Cordani U., Schobbenhaus C., Maurer V.C. 2021b. New U-Pb age to the Pedra Pintada Suite at the type-locality, Roraima, Guiana Shield. In: Congresso Brasileiro de Geologia, 50, 2, 481. Available online at: <https://50cbg.com/anais/> / (accessed on 13 January 2022).
- Rodrigues V.O., Macambira M.J.B. 2021. Evolução geológica e geocronologia U-Pb do Complexo Metamórfico Rio Urubu, Escudo das Guianas, região central de Roraima. In: Congresso Brasileiro de Geologia, 50, 2, 466. Available online at: <https://50cbg.com/anais/> / (accessed on 10 January 2022).
- Santos J.O.S., Hartmann L.A., Gaudette H.E., Groves D.I., McNaughton N.J., Fletcher I.R. 2000. A new understanding of the provinces of the Amazon Craton based on integration of field mapping and U-Pb and Sm-Nd geochronology. *Gondwana Research*, 3(4), 453-488. [https://doi.org/10.1016/S1342-937X\(05\)70755-3](https://doi.org/10.1016/S1342-937X(05)70755-3).
- Santos J.O.S. 2003. Geotectônica dos Escudos das Guianas e Brasil - Central. In: Bizzi L.A., Schobbenhaus C., Vidotti R.M., Gonçalves J.H. Geologia, tectônica e recursos minerais do Brasil: texto, mapas e SIG. Escala 1:2.500.000. Brasília, CPRM, p. 169-226. Available online at: <https://rigeo.cprm.gov.br/handle/doc/5006> / (accessed on 13 January 2022).
- Santos J.O.S., Potter P.E., Reis N.J., Hartmann L.A., Fletcher I.R., McNaughton N.J. 2003. Age, source and regional stratigraphy of the Roraima supergroup and Roraima-like sequences in northern South America, based on U-Pb geochronology. *Geological Society of America Bulletin*, 115(3), 331-348. [https://doi.org/10.1130/0016-7606\(2003\)115<0331:ASARSO>2.0.CO;2](https://doi.org/10.1130/0016-7606(2003)115<0331:ASARSO>2.0.CO;2).
- Santos J.O.S., Breemen O.B.V., Groves D.I., Hartmann L.A., Almeida M.E., McNaughton N.J., Fletcher I.R. 2004. Timing and evolution of multiple Paleoproterozoic magmatic arcs in the Tapajós Domain, Amazon Craton: constraints from SHRIMP and TIMS zircon, baddeleyite and titanite U-Pb geochronology. *Precambrian Research*, 131(1-2), 73-109. <https://doi.org/10.1016/j.precamres.2004.01.002>.
- Santos J.O.S., Hartmann L.A., Faria M.S.G., Riker S.R.L., Souza M.M., Almeida M.E. 2006a. A compartimentação do Cráton Amazonas em Províncias: avanços ocorridos no período 2002-2006. In: Simpósio de Geologia da Amazônia, 9, 156-159.
- Santos J.O.S., Faria M.S.G., Riker S.R.L., Souza M.M., Hartmann L.A., Almeida M.E., McNaughton N.J., Fletcher I.R. 2006b. A faixa colisional K'Mudku (idade Grenvilliana) no norte do Cráton Amazonas: reflexo intracontinental do orógeno Sunsás na margem ocidental do cráton. In: Simpósio de Geologia da Amazônia, 9.
- Santos J.O.S., Rizzotto G.J., Potter P.E., McNaughton N.J., Matos R.S., Hartmann L.A., Chemale F., Quadros M.E.S. 2008. Age and autochthonous evolution of the Sunsás Orogen in West Amazon Craton based on mapping and U-Pb geochronology. *Precambrian Research*, 165(3-4), 120-152. <https://doi.org/10.1016/j.precamres.2008.06.009>.
- Schobbenhaus C., Hoppe A., Lork A., Baumann A. 1994. Idade U/Pb do magmatismo Uatumã no norte do Cráton Amazônico, Escudo das Guianas (Brasil): primeiros resultados. In: Congresso Brasileiro de Geologia, 38, 395-397. Available online at: <http://www.sbge.org.br/home/pages/44#AnaisCongressosBrasileirosdeGeologia> / (accessed on 10 January 2022).
- Spector A., Grant F. S. 1970. Statistical models for interpreting aeromagnetic data. *Geophysics*, 35(2), 293-302. <https://doi.org/10.1190/1.1440092>.
- Tassinari C.C.G., Macambira M.J.B. 1999. Geochronological provinces of the Amazonian Craton. *Episodes*, 22(3), 174-182. <https://doi.org/10.18814/epiugs/1999/v22i3/004>.
- Tassinari C.C.G., Macambira M.J.B. 2004. A evolução tectônica do Cráton Amazônico. In: Mantesso Neto, V., Bartorelli, A., Carneiro, C.D.R.,

- Neves, B.B.B. O desvendar de um continente: a moderna geologia da América do Sul e o legado da obra de Fernando Flávio Marques de Almeida. São Paulo, Beca, p. 471-486. Available online at: <https://geologia.ufc.br/wp-content/uploads/2016/02/geologia-do-continente.pdf> (accessed on 10 January 2022).
- Teixeira W. 1978. Significação tectônica do magmatismo anorogênico básico e alcalino na região amazônica. MSc Dissertation, Universidade de São Paulo, São Paulo, 87 p. <https://doi.org/10.11606/D.44.1978.tde-02042015-141224>.
- Teixeira W., Reis N.J., Bettencourt J.S., Klein E.L., Oliveira D.C. 2019. Intraplate proterozoic magmatism in the Amazonian Craton reviewed: Geochronology, Crustal Tectonic and Global Barcode Matches. In: Srivastava R.K., Erns, R.E., Peng P. Dyke Swarms of the world: a modern perspective. Springer, Singapura, p. 111-154. https://doi.org/10.1007/978-981-13-1666-1_4.
- Trouw R.A.J., Passchier C.W., Wiersma D.J. 2009. Atlas of Mylonites and related microstructures. Springer-Verlag, Berlin, 322 p. <https://doi.org/10.1007/978-3-642-03608-8>.